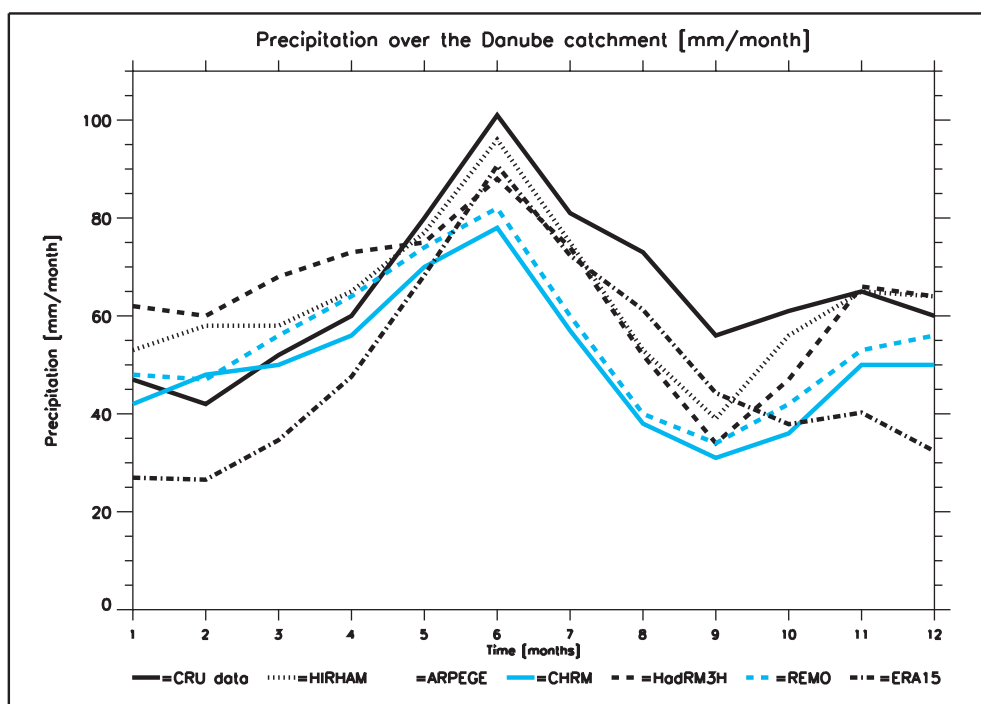




Report No. 338



Intercomparison of water and energy budgets simulated by regional climate models applied over Europe

by

Stefan Hagemann • Bennert Machenhauer
Ole Bøssing Christensen • Michel Déqué
Daniela Jacob • Richard Jones • Pier Luigi Vidale

Hamburg, June 2002

Authors

Stefan Hagemann
Daniela Jacob

Max-Planck-Institut für Meteorologie
Hamburg, Germany

Bennert Machenhauer
Ole Bøssing Christensen

Danish Meteorological Institute
Climate Research Division
Copenhagen, Denmark

Michel Déqué

Météo-France CNRM/GMGEC/EAC
Toulouse, Cedex, France

Richard Jones

Met Office Hadley Centre, Bracknell, UK

Pier Luigi Vidale

Climate Research ETH, Zürich, Switzerland

Max-Planck-Institut für Meteorologie
Bundesstrasse 55
D - 20146 Hamburg
Germany

Tel.: +49-(0)40-4 11 73-0
Fax: +49-(0)40-4 11 73-298
e-mail: <name>@dkrz.de
Web: www.mpimet.mpg.de

INTERCOMPARISON OF WATER AND ENERGY BUDGETS SIMULATED BY REGIONAL CLIMATE MODELS APPLIED OVER EUROPE

STEFAN HAGEMANN^{1*}, BENNERT MACHENHAUER², OLE BØSSING CHRISTENSEN², MICHEL DÉQUÉ³, DANIELA JACOB¹, RICHARD JONES⁴, AND PIER LUIGI VIDALE⁵

¹ Max Planck Institute for Meteorology, Bundesstraße 55, D-20146 Hamburg, Germany

² Danish Meteorological Institute, Climate Research Division, Lyngbyvej 100, DK-2100 Copenhagen Ø, Denmark

³ Météo-France CNRM/GMGEC/EAC, 42 Avenue Coriolis, 31057 Toulouse Cedex 01, France

⁴ Met Office Hadley Centre, London Road, Bracknell, RG12 2SY, UK

⁵ Climate Research ETH, Winterthurerstrasse 190, 8057 Zürich, Switzerland

* e-mail: Hagemann@dkrz.de
<http://www.mpimet.mpg.de/~hagemann.stefan>
Tel.: +49-40-41173-101
Fax: +49-40-41173-366

June 2002

ISSN 0937-1060

Contents

Abstract	3
1. Introduction	3
2. The regional climate models	4
2.1. HIRHAM	4
2.2. ARPEGE	5
2.3. CHRM	6
2.4. HadRM3H	6
2.5. REMO	7
3. Estimation of biases in the water and energy balance	8
4. The Danube catchment	10
4.1. Intercomparison between the models	12
4.2. Water and energy balances	16
4.2.1. HIRHAM	16
4.2.2. ARPEGE	20
4.2.3. CHRM	21
4.2.4. HadRM3H	22
4.2.5. REMO	22
5. The Baltic Sea catchment	28
5.1. Intercomparison between the models	28
5.2. Water and energy balances	33
5.2.1. HIRHAM	33
5.2.2. ARPEGE	33
5.2.3. CHRM	34
5.2.4. HadRM3H	34
5.2.5. REMO	35
6. Conclusions	41
References	42

Abstract

This study presents a model intercomparison of four regional climate models (RCMs) and one variable resolution atmospheric general circulation model (AGCM) applied over Europe with a special focus on the hydrological cycle and the surface energy budget. The models simulated the 15 years from 1979 to 1993 by using quasi-observed boundary conditions derived from ECMWF re-analyses. The model intercomparison focuses on two large catchments which represent two different climate conditions and that cover two areas of major research interest within Europe. The first is the Danube catchment which represents a continental climate that is dominated by advection from the surrounding land areas, and it is used to analyse the common model error of a too dry and too warm simulation of the summertime climate of south-eastern Europe. This summer warming and drying problem is seen in many RCMs, and to a less extent in GCMs. The second area is the Baltic Sea catchment which represents maritime climate dominated by advection from the ocean and from the Baltic Sea. This catchment is a research area of many studies within Europe as it is also covered by the BALTEX program.

For all models, the mean monthly biases of all components of the hydrological cycle over land are estimated, and the mean monthly deviations of the surface energy fluxes from ECMWF re-analysis data are computed. An evaluation of these biases and deviations suggests possible sources of error in each of the models. For the Danube catchment, systematic errors in the dynamics are causing the prominent summer drying problem for three of the RCMs, while for the fourth RCM this is related to deficiencies in the land surface parameterization. The AGCM does not show this problem. For the Baltic Sea catchment, all models similarly overestimate the precipitation throughout the year except during the summer. This model deficit is probably caused by the internal model parameterizations, such as the large-scale condensation and the convection schemes.

Keywords: regional climate model intercomparison, hydrological cycle, surface energy fluxes, biases

1. Introduction

The EU project MERCURE (Modelling European Regional Climate: Understanding and Reducing Errors) was launched to improve regional climate models by understanding and reducing sources of errors, notably those arising through poor parameterization of physical processes and insufficient model resolution. Several European partners have participated with their regional climate models (RCMs) in the MERCURE project. The HIRHAM4 high resolution limited area model (*Christensen et al.*, 1996) was used by two of the partners, DMI (Danish Meteorological Institute) and MPI (Max-Planck-Institute for Meteorology). Here, a close, long-lasting cooperation between DMI and MPI in EU supported regionalization projects (*Machenhauer et al.*, 1996, 1998) was continued. The ARPEGE model (*Déqué et al.*, 1998) was used by Météo-France, a modified version of the German Weather Service's forecast Europa model (CHRM; *Lüthi et al.*, 1996) was used by the Institute for Climate Research of the ETH Zurich, and the HadRM3H model (*Jones et al.*, 1995) was used by the Hadley Centre.

This study presents a model intercomparison of the models that have participated in the MERCURE project plus the REMO model developed at MPI (*Jacob*, 2001) with a special

focus on the hydrological cycle and the surface energy budget. Involving the REMO model in the study adds an interesting dimension as it shares the dynamical core of the CHRM model and the physics of the HIRHAM model. 15 years model simulations covering the time from 1979 to 1993 were compared. In order to minimize the influence of errors in the prescribed SSTs and the lateral boundary conditions, these were determined from ECMWF re-analysis data (ERA; Gibson *et al.*, 1997) for all models except for the ARPEGE model which used only prescribed SSTs as it is a global model using a stretched model grid with a high resolution over Europe (cf. Sect. 2.2).

For the model intercomparison two large European catchments were chosen which represent two different climate conditions. The Danube catchment represents continental climate as it is *land-dominated* by advection from the surrounding land areas, the Baltic Sea catchment represents maritime climate since it is *water-dominated* by advection from the ocean and from the Baltic Sea. It is of interest to see whether the model behaviour and their systematic errors are similar for both climate regions and how differently the model respond to the systematic errors.

Previous analysis of some of the models has shown that common systematic errors in the RCMs and their driving GCMs can explain some of the biases in the 2m-temperature and the precipitation (Machenhauer *et al.*, 1996, 1998). A special model feature that is typical for many RCMs, and to a less extent is visible in some GCMs, is the too dry and too warm simulation of climate over south-eastern Europe during the summer (Machenhauer *et al.*, 1998). These studies showed that this bias could not be explained by systematic errors in the large scale general circulation. Thus, one major task in MERCURE was to understand and reduce or eliminate this model error referred to as the summer drying problem in the following. Hence, this study focuses on the Danube catchment, a large drainage basin contained in the area where this problem occurs.

The second focus of this study is the Baltic Sea catchment which is an area of high research interest within Europe intending to understand and describe its climate and the components of the water and energy budgets (e.g., see Bengtsson, 2001). This area is also covered by the Baltic Sea Experiment (BALTEX) (cf. BALTEX, 1995) which is a European sub-program of the ‘Global Energy and Water Cycle Experiment’ (GEWEX; WMO, 1988).

Sect. 2 gives a short overview of the participating RCMs. In Sect. 3, the methods are described that were used to compute the water and energy balances at the land surface and the biases in the hydrological cycle. Sect. 4 focuses on the Danube catchment and Sect. 5 on the Baltic Sea catchment.

2. The regional climate models

2.1. HIRHAM

The regional climate model HIRHAM4 (Christensen *et al.*, 1996) is based on the HIRLAM (High Resolution Limited Area Model) short-range weather prediction model (Källén, 1996). In order to make a model that is suitable for long climate integrations with lateral boundary conditions taken from the MPI global climate model ECHAM4 (Roeckner *et al.*, 1996), the physical parameterization of the ECHAM4 model has been incorporated into the regional

model. HIRHAM4 is a standard Eulerian primitive-equation staggered grid point model with additionally a prognostic cloud water equation (as in ECHAM4). The model has an arbitrary number of vertical hybrid levels, at present 19 levels similar to those adopted in ECHAM4. A linear fourth-order horizontal diffusion scheme is applied, but in mountainous regions it is switched off for temperature and humidity in order to avoid spurious mixing of air masses from different levels causing unphysical precipitation. The model is applied with a lateral boundary relaxation zone, currently 10 points wide, following *Kållberg and Gibson (1977)* with a quasi-exponential relaxation function for most prognostic variables. In order to avoid reflection of gravity waves from the upper boundary, a 5-layer sponge filter (*Shapiro, 1970*) is applied for temperature, wind, and specific humidity.

The land surface parameterization scheme in HIRHAM4 (the same as in ECHAM4) uses five soil temperature layers and one moisture layer (bucket). Soil temperatures are computed solving the heat conduction equation using soil characteristics depending on texture. Surface runoff is calculated using the Arno scheme, taking into account sub-grid scale effects due to the heterogeneity within a gridbox (*Dümenil and Todini, 1992*). Furthermore, deep soil drainage is computed. The global dataset of fields of land surface parameters used in the surface scheme is based upon *Hagemann et al. (1999)* and *Hagemann (2002)* who constructed their dataset from a 1 km global distribution of major ecosystem types. Orography and orography related surface fields are used according to *Christensen et al. (2001)* which are based on 1 km resolution satellite data.

Several changes were made to the HIRHAM4 model presented by *Christensen et al. (1996)* during the MERCURE project which are described in *Hagemann et al. (2001)*.

The HIRHAM model grid used in the present study covers an area including the whole of Europe and part of the Atlantic Ocean. A rotated lat-long grid is used with a resolution of 0.44 degrees (about 50 km).

2.2. ARPEGE

The ARPEGE-IFS model is an atmosphere model developed by the French Meteorological Service Météo-France and the European Centre for Medium-range Weather Forecasts (ECMWF) for operational short- and medium-range forecasting. A climate version of this model is developed at Météo-France (*Déqué et al., 1998*). This version uses a spectral T106 truncation. The associated grid has 120 pseudo-latitudes and 240 pseudo-longitudes. The pole of the new system of coordinates is located in the Mediterranean sea. The equations are discretized on an isotropic grid. The antipode is located in the southern Pacific ocean. A stretching factor is applied as a function of the pseudo latitude. The maximum value is 3 at the Mediterranean pole, the minimum is 1/3 at the opposite pole. Thus the resolution over Europe is between 50 and 70 km. The vertical resolution uses 31 levels. The physical parameterizations have no strong originality: radiation including indirect effect of aerosols, convection by a mass flux scheme with moisture convergence closure, gravity wave drag with resonance, block, and lift effect, soil processes including a parameterization of the snow age. The cloud-precipitation-vertical diffusion scheme uses a simple turbulent scheme to diagnose the probability distribution of water inside the model mesh.

2.3. CHRM

The Climate High Resolution Model (CHRM) is fundamentally a climate version of the operational mesoscale weather forecasting model of the German and Swiss meteorological services, the HRM (High Resolution Model), previously known as EM (Europa Modell, *Majewski and Schrodin, 1994, Lüthi et al., 1996*). The model grid is a regular latitude/longitude grid (Arakawa type C) with a rotated pole and a hybrid vertical coordinate (*Simmons and Burridge, 1981*) with 20 levels. It includes a full package of physical parameterizations, including a mass-flux scheme for moist convection (*Tiedtke, 1989*), Kessler-type microphysics (*Kessler, 1969, Lin et al., 1983*), a radiation package including interaction with partial cloud cover (*Ritter and Geleyn, 1992*), a land surface scheme (*Dickinson, 1984*) with three soil layers, interception and snow (*Jacobsen and Heise, 1982*), vertical diffusion and turbulent fluxes based on the flux-gradient approach (*Mellor and Yamada, 1974*).

CHRM is nudged at the lateral boundaries using the *Davies (1976)* technique for temperature, moisture and wind, every six hours, while the bottom boundary conditions are only initialized and not nudged, so that the soil vegetation atmosphere transfer scheme (SVATS) is allowed to develop its own solution over the course of the climate simulation. The only substantial deviations from the original numerical weather prediction model, which is normally driven by the GCM of the German Weather Service (GME, *Majewski et al., 2001*), are due to the use of ERA data for the lateral boundaries forcing; the nature of the climate simulations, which require more careful specification of the soil model framework and of the yearly evolution of surface and sub-surface parameters and processes; the use of the *Beljaars and Viterbo (1998)* surface layer parameterization.

Three soil moisture levels (10, 35, 120 cm) are used (and equivalent depths for the force-restore thermal layers, through the use of appropriate time constants) and are initialized with ERA data, retaining a climatological layer from 1.6 to 3.2m, which serves as a fixed boundary condition, only accessed in case the root zone layer should dry further than the air dryness point. In terms of soil thermal processes, the original extended force-restore method of *Jacobsen and Heise (1982)* was modified to include a representation of soil moisture freezing, similar to *Lunardini (1983)*, corresponding to a latent heat release/uptake barrier in a 1 degree interval around the freezing point, as is also done in the BATS 1e (*Dickinson et al., 1993*) and LSM (*Bonan, 1996*) SVATS. The state of the vegetation, as described by LAI, roughness and fraction of green vegetation is specified in time and space by assimilating data from the ISLSCP CD-ROM (*Sellers et al., 1994*), with a spatial resolution of 1 degree and a time resolution of 1 month.

The use of *Beljaars and Viterbo (1998)* in lieu of the more standard *Louis et al. (1982)* surface layer parameterization was motivated from a well-known model cold bias, from improvements discussed in that paper and from experience with other numerical models (RAMS, CSU GCM), but did not show to have sufficient impact on the simulations when compared, for instance, to options in the convection or the land surface parameterizations.

2.4. HadRM3H

HadRM3H is the limited area higher resolution version of the AGCM HadAM3H which itself is an improved version of HadAM3, the atmospheric component of the latest Hadley Centre coupled AOGCM, HadCM3. HadAM3 is described in *Pope et al. (2000)* and is a gridpoint

model, generally run at $2.5^\circ \times 3.75^\circ$ resolution, which contains all the usual representations of atmospheric and land surface physics (some of which are described in more detail below).

The modifications introduced to form HadAM3H are described in *Murphy et al. (2002)* and are summarised briefly here: The horizontal resolution is doubled in both directions; A scheme to treat the radiative effects of anvil cirrus in deep convective regimes (*Gregory, 1999*) is included; The threshold relative humidity for cloud formation within a gridbox (RH_{crit}) has been parameterized (*Cusack et al., 1999*); The cloud scheme is now such that cloud fraction is 0.6 rather than 0.5 when the gridbox specific humidity (which is assumed to have sub-grid variability) reaches saturation; Various changes relating to the conversion of cloud water to precipitation to generate a realistic radiation balance; A fully interactive sulphur cycle is included together with the representation of the first indirect effect of sulphate aerosols; The fraction of a grid box on which precipitation falls is adjusted to take account of the increase in resolution; A full radiative coupling of the vegetation canopy to the soil surface is introduced.

HadRM3H then uses an identical formulation to HadAM3H except where explicit account must be taken of the impact of higher resolution on the representation of physical and dynamical processes. The resolution is increased to 0.44° which with the rotated coordinate system provides a quasi-uniform linear resolution of 50km (150 km over Europe in HadAM3H). The vertical resolution is unchanged at 19 levels. Changes have been made to the RH_{crit} parametrization to allow for the fact that at higher horizontal resolution more of the spectrum of atmospheric motions are resolved and that the relationship between the variability of humidity at and below the grid scale changes. Also, due to the change in precipitation intensities seen at higher resolution the fractional area of the gridbox over which this is assumed to fall is further changed. Driving this model with HadAM3H provides simulations which are consistent over large scales.

One important aspect of the models described above is their use of MOSES, the new land surface scheme developed by *Cox et al. (1999)*. Both soil moisture and temperature are modelled in four soil layers and soil moisture is available for evapotranspiration in a root zone whose depth is dependent on vegetation type. The scheme also includes a representation of the freezing and melting of soil moisture, leading to better simulations of surface temperatures, and a new formulation of evaporation which includes the dependence of stomatal resistance on temperature, vapour pressure deficit and CO_2 .

2.5. REMO

The regional climate model REMO (*Jacob, 2001*) is based on the Europamodell/ Deutschlandmodell system (*Majewski and Schrodin, 1994*). REMO may use two different physical parameterization schemes - the original one called DWD-physics or the ECHAM4-physics from the MPI global climate model ECHAM4 (*Roeckner et al., 1996*) which was used in this study. The dynamical scheme is in both cases identical.

REMO uses a rotated spherical Arakawa-C-grid. The model has an arbitrary number of vertical hybrid levels, at present 20 levels. A linear fourth-order horizontal diffusion scheme is applied to momentum, temperature and water content. A Leap-frog time stepping with semi-implicit correction and Asselin-filter is used. The model is applied with a lateral boundary formulation following *Davies (1976)* which adjusts the prognostic variables in a boundary zone of 8 grid boxes.

Vertical diffusion and turbulent surface fluxes are calculated from Monin-Obukhov similarity theory (Louis, 1979) with a higher order closure scheme for the transfer coefficients of momentum, heat, moisture, cloud water within and above the PBL. The eddy diffusion coefficients are calculated as functions of the turbulent kinetic energy. The land surface parameterization scheme in REMO is the same as for HIRHAM (see Sect. 2.1) except for the fact that the land surface parameters fields used in the surface scheme are only based upon Hagemann *et al.* (1999), and the orographic roughness length is computed using a method of Heise (personal communication, 2000).

The REMO model grid used in the present study covers an area including the whole of Europe and part of the Atlantic Ocean. A rotated lat-long grid is used with a resolution of 0.5 degrees (about 55 km).

3. Estimation of biases in the water and energy balance

In order to estimate the biases of the components of the simulated hydrological cycle, the corresponding observed values have to be known. The water balance at the land surface is described by

$$P - E - R = \Delta WS = \frac{\Delta W + \Delta S}{\Delta t} \quad (1)$$

P is precipitation, E is evapotranspiration, R is the total runoff occurring at the land surface and ΔWS is the change in the water storage of the soil moisture reservoir ΔW and the accumulated snowpack ΔS within a certain time period Δt . In this study, monthly values will be considered so that $\Delta t = 1$ month. An observed precipitation P_{obs} can be taken from the CRU precipitation dataset (Hulme *et al.*, 1995). But the other components of Eq. (1) are usually not available as observations. Thus, these values have to be estimated.

The total runoff is closely connected to the river discharge for which observed values are commonly available for many catchments. In hydrology, so-called rainfall-runoff models are often used to derive the discharge of a catchment from time series of precipitation. These models are catchment-related and require long time series (usually daily values) of observed precipitation and discharge for their calibration. However, adequate observations are not available for many catchments, so we have developed an estimation approach that does not require the availability of these kind of observations. As observed monthly discharge data are commonly available for many rivers we wanted to find a way to estimate the "observed" total runoff from observed monthly values of discharge.

The idea is to establish a statistical relation (Eq. (2)) between model computed monthly ensemble mean values of total runoff within a specific catchment (here the Danube and the Baltic Sea catchment) and model computed monthly ensemble mean values of discharge from that catchment based on the HIRHAM model simulation and the Hydrological Discharge (HD) model (Hagemann and Dümenil, 1999). Having established such a relation it is then used to obtain corresponding quasi-observed values of runoff from observed values of discharge. The HD model separates the lateral water flow into the three flow processes of overland flow, base flow, and river flow. Overland flow uses surface runoff as input, baseflow is fed by drainage from the soil and the inflow from other grid boxes contributes to riverflow. The sum of the

three flow processes is equal to the total outflow from a grid box. As a general strategy, the HD model computes daily discharge at a latitude-longitude grid with 0.5° resolution. The model input fields of runoff and drainage resulting from the various (global or regional) general circulation model resolutions are therefore interpolated to the same 0.5° grid. In this study, the runoff and drainage fields of the HIRHAM simulation (cf. Sect. 2.1) were used to obtain the simulated discharge.

For a certain catchment, we assume that the relation between runoff R and discharge D can be approximated by Eq. (2) where L is an average lag time between R and D and the factor a is approximating a smoothing with time.

$$D(t) = a(t) \cdot R(t - L) \quad (2)$$

Optimum values of L and a_i were determined for each of the 12 calendar months from the 15 years time series of monthly total runoff and discharge values using a least square fit, allowing for integer lag values only. For the Danube catchment as well as for the Baltic Sea catchment, an optimum lag value $L = 1$ month was found. Thus, Eq. (2) becomes

$$D_i = a_i \cdot R_{i-1} \quad (3)$$

for month i . Assuming that Eq. (3) with the model determined a_i is valid also for observed values of discharge and runoff a set of 12 quasi-observed runoff ensemble mean values, R_{obs} , can be estimated from the observed long term mean discharge values available.

Next, for the estimation of the monthly storage changes ΔWS , a similar statistical method was chosen as for the runoff. As these storage changes largely depend on the precipitation we approximate this relation by

$$\Delta WS_i = b_i \cdot P_i \quad (4)$$

Here, again we determine the coefficients b_i for each of the 12 calendar months from the 15 years time series of monthly ΔWS and P of the corresponding RCM, e.g. the HIRHAM model, by a least square method. In order to obtain quasi observed ΔWS values, ΔWS_{obs} , from observed P values the model determined relation between ΔWS and P is assumed to be valid also in reality. Using Eq. (4), we can then estimate the ΔWS_{obs} from the CRU precipitation data, P_{obs} . In this way, a quasi-observed evapotranspiration E_{obs} was estimated by inserting P_{obs} , R_{obs} and ΔWS_{obs} into Eq. (1). The so determined observed and quasi observed values were finally used to determine biases for each model simulation.

Since in particular Eq. (4) is dependent on the realism of the model used for its derivation and it is easily computed for other models than the HIRHAM model we have computed ΔWS_{obs} values using b_i in Eq. (4) determined from each of the models included in the intercomparison. In the following the estimated bias of the evapotranspiration is called $Bias(E)$ if the coefficients in Eq. (4) are determined from the model in question whereas it is called $Bias(EQ)$ if the b_i used are determined from the HIRHAM model.

For an atmospheric column, the water balance is expressed by

$$E - P + C = \frac{\Delta Q}{\Delta t} \quad (5)$$

C is the lateral convergence (divergence if C is negative) of moisture into the column, and $\frac{\Delta Q}{\Delta t}$ is the change of atmospheric moisture content (precipitable water) in the column within a time period Δt (here one month). It is assumed that the bias in this change from month to month is negligible compared to the biases of the other variables in Eq. (5). The deviation of the different simulated monthly changes in precipitable water from ERA data are small compared to the computed biases in P and E so that the assumption seems to be justified. Thus, Eq. (6) becomes valid for the biases.

$$Bias(C) = Bias(P) - Bias(E) \quad (6)$$

When $Bias(EQ)$ is used in this balance instead of $Bias(E)$ the corresponding convergence bias is called $Bias(CQ)$.

It can be summarized that the E estimate is residual from measured P , inferred runoff (from measured discharge) and inferred ΔWS (from measured P). The estimated convergence bias is residual from the P bias and the estimated E bias, and thus the convergence bias can be written as a function of the bias in estimated runoff and water store (hence a function of discharge and P). Note that one can get a direct C estimate from ERA data over the region by performing an assimilation experiment (as in Jones *et al.*, 2002).

For the energy balance, appropriate catchment scale observations were not available at the time of the study. Thus, deviations of the simulated energy fluxes from ERA data are computed instead. One has to bear in mind that these data are also some kind of model data, although influenced more or less by the available observations in the ERA data-assimilation system. For longer time periods (such as a year), the energy balance at the land surface can be expressed by

$$LHF + SHF + SR + TR = 0 \quad (7)$$

LHF is the latent heat flux, SHF is the sensible heat flux, SR is the surface solar radiation and TR is the surface thermal radiation. All fluxes are positive downward and negative upward. Beside deviations of model values from the ERA values of these components of the energy balance we shall consider also such deviations of model evapotranspiration. We call such deviations $Bias(ER)$ and the corresponding convergence biases are called $Bias(CR)$.

4. The Danube catchment

The location of the Danube catchment is shown in Fig. 1. Its area comprises about 807000 km² and an annual mean discharge of 6435 m³/s (203 km³/a) is observed at a measurement station near the mouth of the river. All the atmospheric variables were integrated over the whole catchment area. Thus, in the following, all the water fluxes will be expressed in mm/month instead of a volume flux unit. In Sect. 4.1, the different simulated variables of all models are directly compared to each other and to observations. The results of this section are summarized in Table 1. The biases in the water balances and the deviations from ERA data in the energy balance are analysed for each model separately in Sect. 4.2. The analysis is described in more detail in the HIRHAM section 4.2.1.

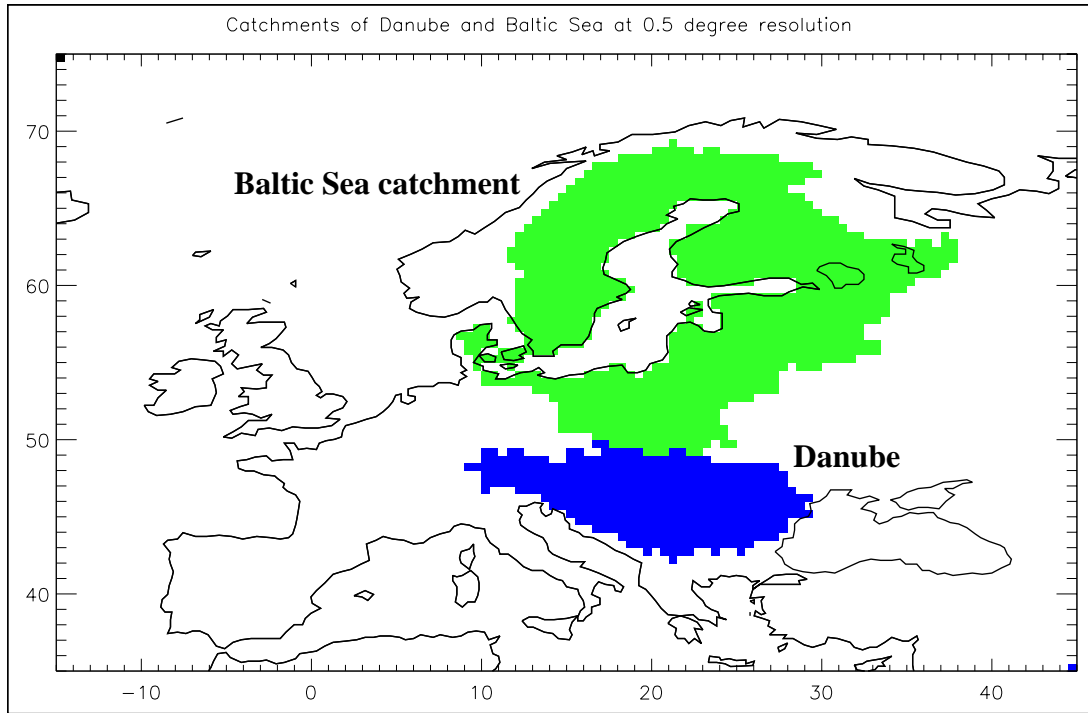


Fig. 1. Catchments of Danube and Baltic Sea at 0.5 degree resolution

Table 1. Overview over regional climate model performance in the Danube catchment.

‘+’ designates overestimation, ‘-’ underestimation, ‘o’ good simulation, and ‘.’ no clear rating possible.

Simulated value		HIRHAM	ARPEGE	CHRM	HadRM3H	REMO
2m temperature	winter	o	o	-	o	o
	spring	o	-	-	o	o
	summer	+	o	o	++	++
	autumn	o	-	-	+	o
Precipitation	winter	+	+	o	+	o
	spring	o	o	o	o	o
	summer	-	o	--	-	--
	autumn	-	o	-	-	-
Evaporation	winter	+	o	o	o	o
	spring
	summer	+	o	-	-	-
	autumn	o	o	-	-	-
Total Runoff	winter	-	-	-	-	-
	spring	--	++	-	o	--
	summer	-	o	o	o	o
	autumn	-	o	-	-	-
Snowpack	winter	-	+	-	-	-
	spring	-	+	o	o	-

4.1. Intercomparison between the models

Fig. 2 shows the simulated precipitation of the models compared to CRU observations. For all models except ARPEGE the summer drying problem can clearly be seen. For ARPEGE, almost no indication of the drying problem exists anymore in the Danube catchment, only June and August have negative precipitation biases. REMO and CHRM show the largest drying problem starting in May and lasting until December. HadRM3H and HIRHAM behave very similarly with negative precipitation biases from June to October. All models except ARPEGE are able to catch the time of the maximum precipitation in June while the latter simulates this maximum one month too early. All models except ARPEGE and REMO are also able to capture the local maximum in November. All models except CHRM and REMO overestimate precipitation in the winter. ARPEGE, HadRM3H and REMO capture the time of the minimum in February.

Fig. 3 shows the differences of the simulated 2m temperature to CRU data. HadRM3H and REMO exhibit a large warm bias ranging from May to October. HIRHAM has a moderate warm bias in August and September while ARPEGE has a small warm bias in July and August. ARPEGE has separate cold biases in the autumn and spring while CHRM is too cold throughout the year except for the summer with maximum cold biases in March and October. Different to the other models that show a summer dry bias in Fig. 2 (HIRHAM, HadRM3H, REMO), CHRM does not have a summer warm bias.

Fig. 4 shows the simulated evapotranspiration compared to ERA data and the quasi-observed evapotranspiration obtained from the HIRHAM run. As the latter is only a rough estimate, the results obtained from this plot have to be considered carefully. Thus, in addition a comparison of the simulated latent heat fluxes to ERA data is also included (see Fig. 5). All models underestimate the evapotranspiration in the summer. This underestimation is comparatively large for CHRM, HadRM3H and REMO. For HadRM3H and REMO, this may intensify their warm biases in the summer. More or less all models tend to overestimate the evapotranspiration in the winter although this seems to be significant only for HIRHAM.

Fig. 6 shows the simulated total runoff compared to the quasi-observed runoff obtained from the HIRHAM simulation. HIRHAM and REMO largely underestimate the runoff, as CHRM does except for the peak in March. In the spring, this is related to the large underestimation of the accumulated snowpack (see Fig. 7). ARPEGE largely overestimates the snowmelt induced runoff in the spring which is related to the large overestimation of the accumulated snowpack. The latter causes also a one month delay of the runoff peak. The one month delay of the HadRM3H runoff peak is related to the fact that almost the whole model runoff is comprised of drainage from the lowest soil layer. In the HadRM3H model, the major part of the snowmelt infiltrates into the soil instead of flowing laterally as surface runoff. CHRM, REMO and HIRHAM capture the time of the runoff peak in March. All models tend to underestimate the total runoff in the winter which may be related to the overestimated evapotranspiration at the same time.

Fig. 8 shows the simulated soil moisture content. As the models use different soil schemes (except for HIRHAM and REMO), one should only compare the variations in the annual cycle of the soil moisture instead of comparing its total amounts. All models except ARPEGE vary similarly and have large variations in the soil moisture during the year. ARPEGE shows a distinct April maximum which is induced by the large snowmelt.

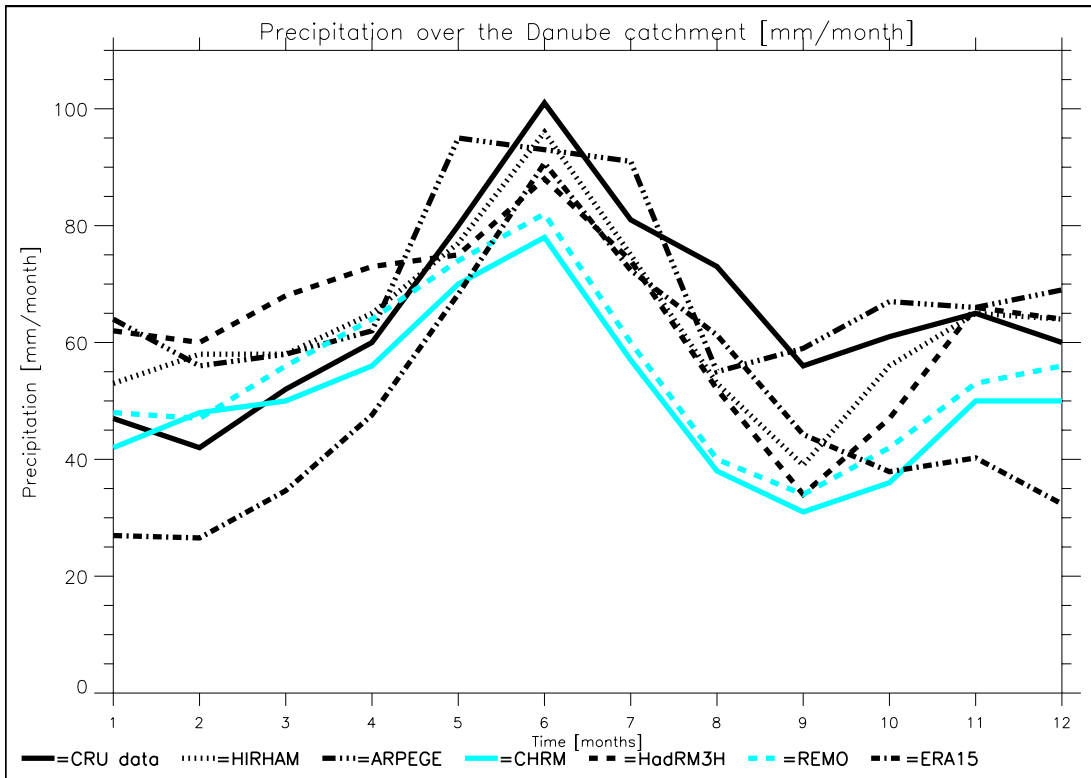


Fig. 2. Precipitation over the Danube catchment in mm/month

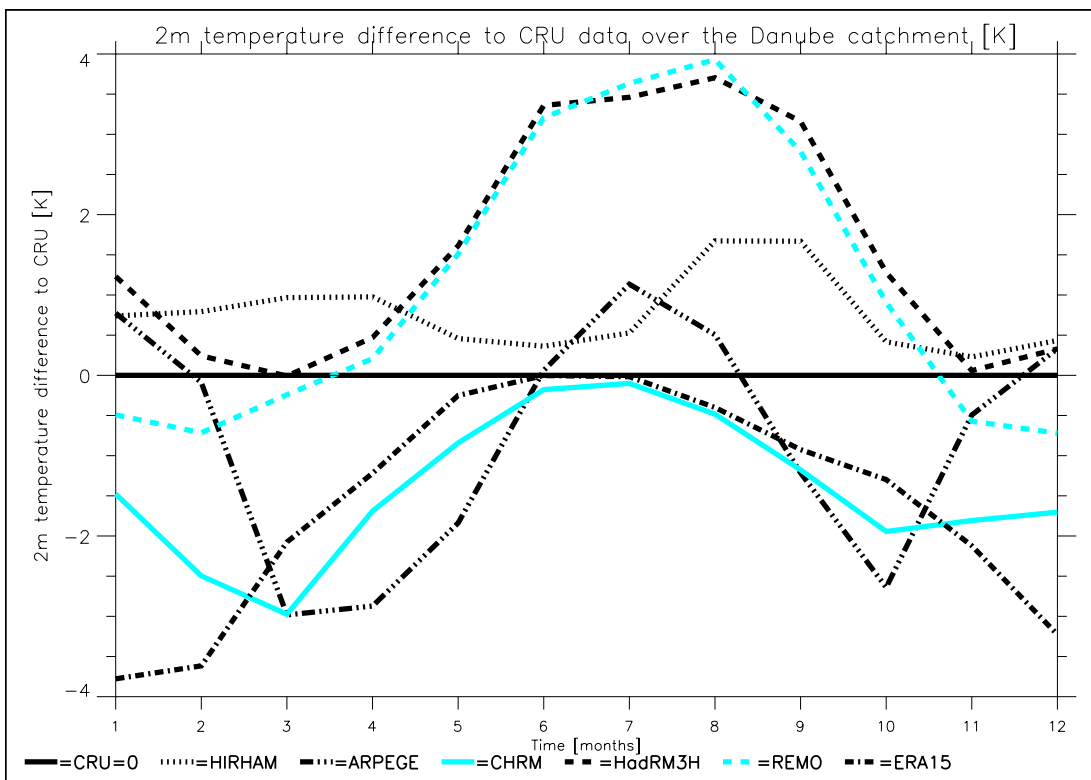


Fig. 3. 2m temperature difference to CRU data over the Danube catchment in K

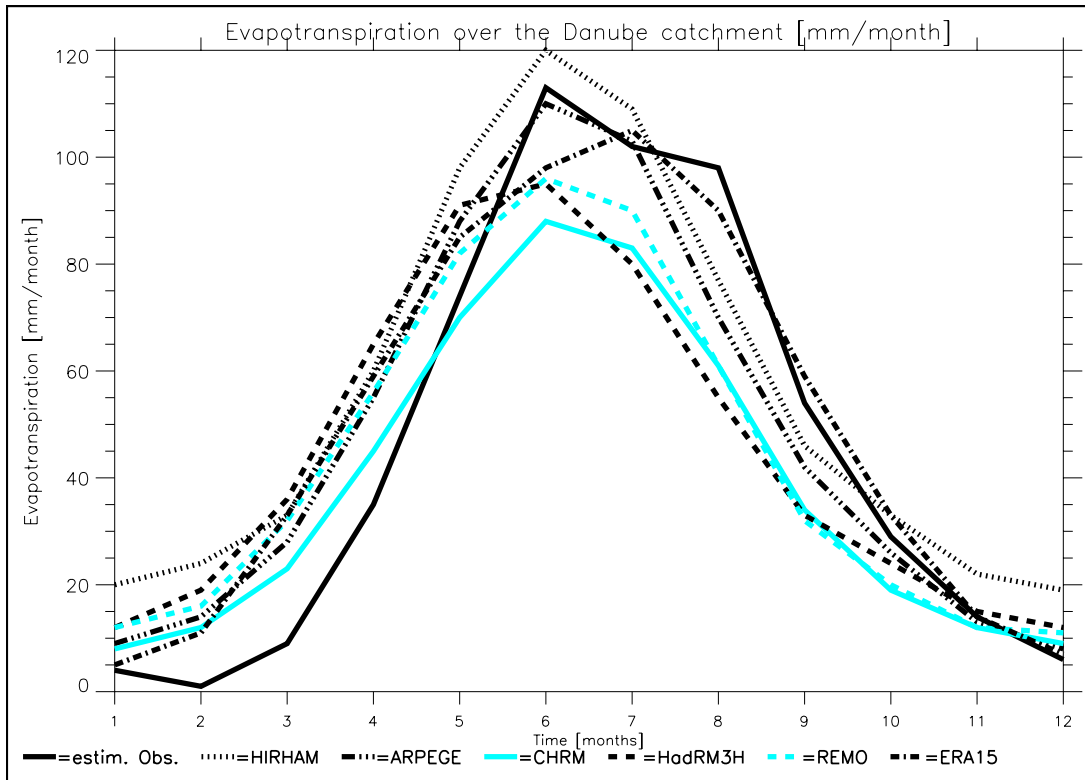


Fig. 4. Evapotranspiration over the Danube catchment in mm/month

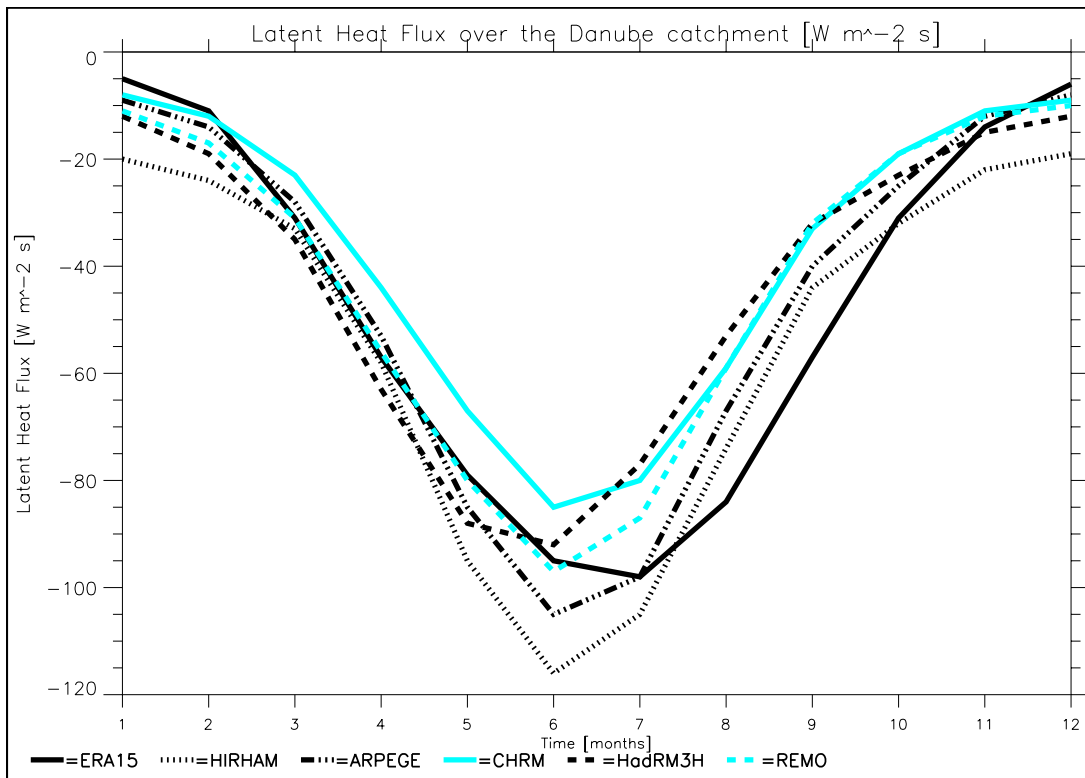


Fig. 5. Latent heat flux over the Danube catchment in $W m^{-2} s$

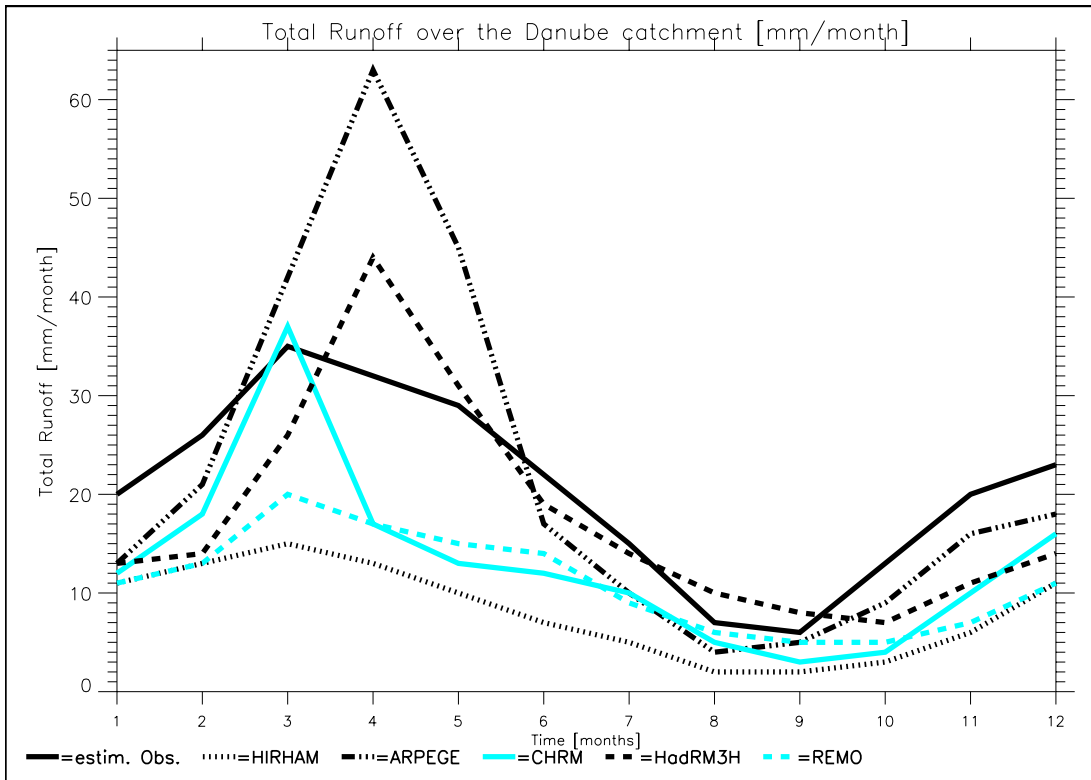


Fig. 6. Total runoff over the Danube catchment in mm/month

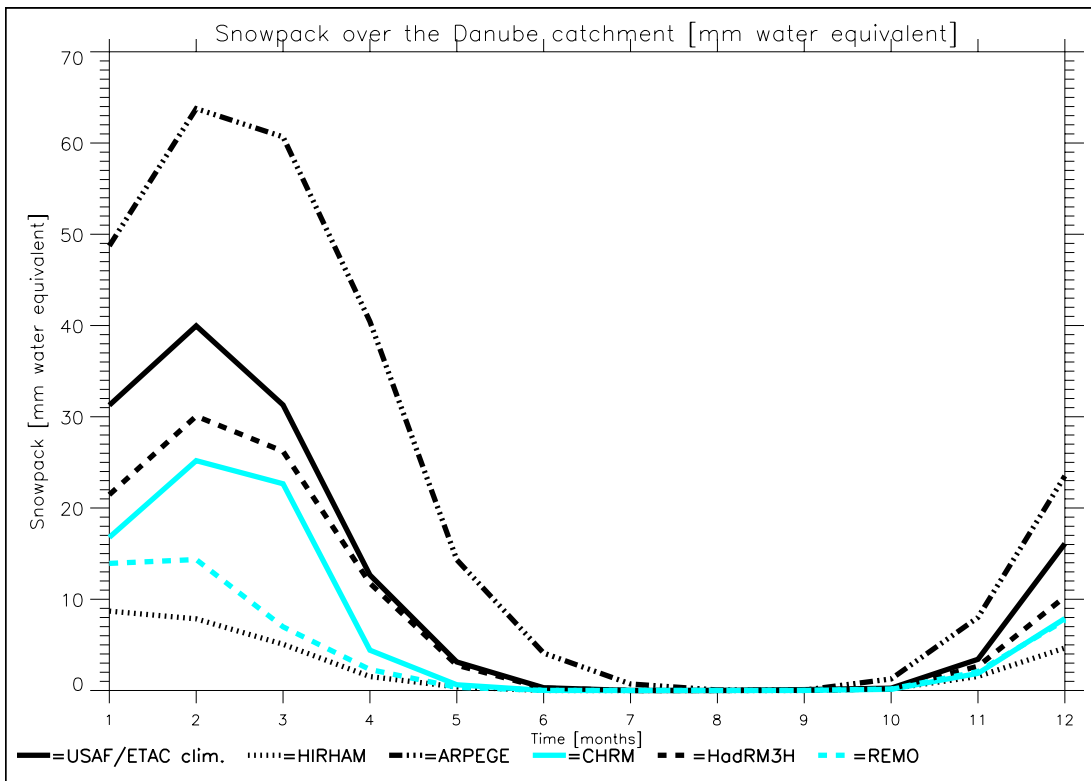


Fig. 7. Mean snow pack over the Danube catchment in mm water equivalent. USAF/ETAC climatological values of Foster and Davy (1988) are used as observed values for comparison.

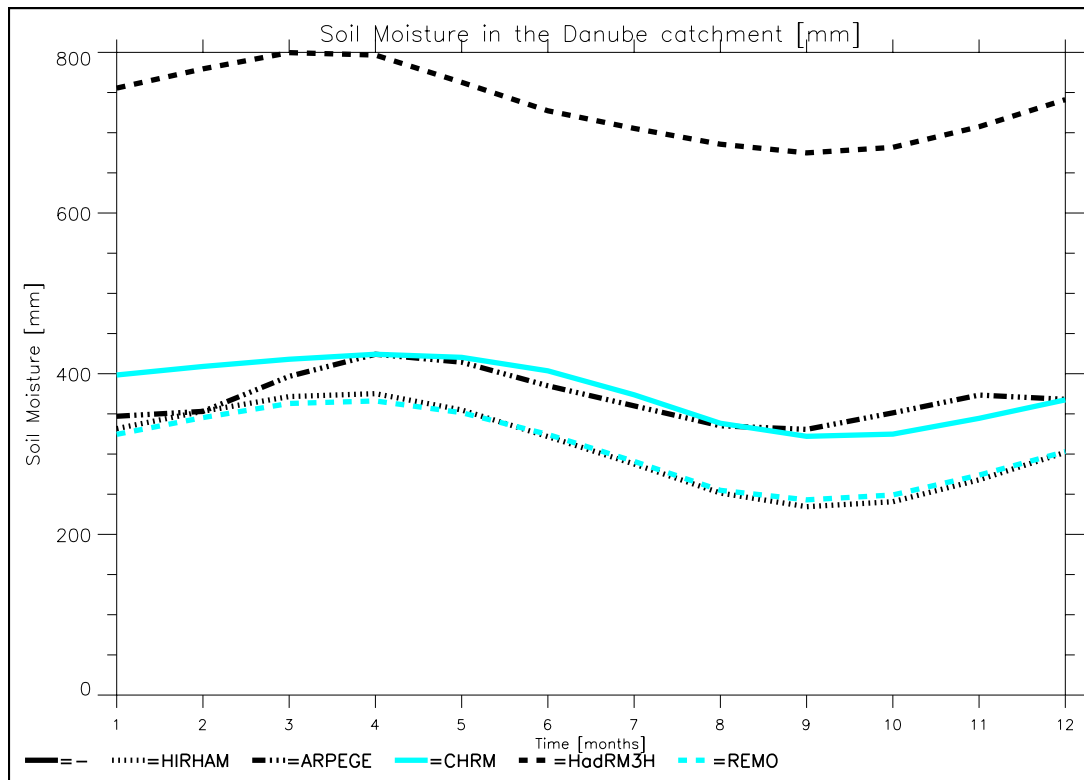


Fig. 8. Mean soil moisture in the Danube catchment in mm

4.2. Water and energy balances

4.2.1. HIRHAM

Fig. 9 shows the estimated biases of the components in the hydrological cycle (Eq. (6)) for the HIRHAM simulation (in mm liquid water per month). For comparison, the values of $Bias(ER)$, and the corresponding $Bias(CR)$ values are also shown as well the estimated biases of ΔWS , determined from model computed ΔWS and quasi observed ΔWS computed from Eq. (4) using HIRHAM derived b_i . The estimated $Bias(E)$ values indicate that the model simulates an excessive evapotranspiration in the beginning of the year. Assuming this is correct the figure indicates furthermore that not all of this excessive moisture supply to the model atmosphere is released locally as excessive precipitation, because it is partly compensated by $Bias(C)$, an excessive divergence of moisture out of the catchment (or excessive inflow of dryer air). During the following months the estimated $Bias(E)$ increases slightly, but after May it decreases, ending up with a negative value in August. Simultaneously, the balancing bias of moisture divergence, $Bias(C)$, increases until May, whereupon it decreases to zero in August. After August $Bias(E)$ increases again as well as the balancing bias of moisture divergence. These estimated variations of the moisture source (evapotranspiration) and the sink (moisture divergence) suggest an explanation of the variation with time of the precipitation bias: it decreases from a positive maximum bias in February to a minimum in August, being negative in the summer period May to October, whereupon it increases again to the February value.

This explanation relies, however, heavily on the estimated bias of the evapotranspiration for which therefore an independent estimate is desirable. Such one, the $Bias(ER)$ curve, is shown also in Fig. 9. Comparing the $Bias(ER)$ curve with the $Bias(E)$ curve we find a good, all over

agreement, including the sign, except in the months February to May. During these months we find relatively small values of $Bias(ER)$ compared to the relatively large values of $Bias(E)$. This constitutes a significant difference between the two estimates in the months February to May (in the following we call these months "the melting period").

An explanation of this difference can be that in our estimate of $Bias(E)$ we have used too small values of the quasi observed E_{obs} determined from Eq. (1), because the ΔWS_{obs} , determined from Eq. (4), and perhaps also the R_{obs} , determined from Eq. (3), are estimated too large. In other words the coefficient b_i in Eq. (4) and perhaps also $1/a_i$ in Eq. (3) seem to be estimated too large. We have used the HIRHAM simulation to determine both sets of coefficients so that errors in their values may be caused by inaccuracies in the HIRHAM model. The main reason seems to be the systematic error in the HIRHAM snowpack, see Fig. 7, namely the unrealistic low snow pack simulated during the winter and thus an unrealistic small snow melt during the spring. This systematic error may have lead to such errors in the determination of both coefficients.

Since too little snowmelt is simulated while P is slightly overestimated, the simulated ΔWS is much larger than it should be. Thus, the b_i derived from Eq. (4) are larger than in reality which results in an overestimation of ΔWS_{obs} . According to Eq. (1) this causes an underestimation of E_{obs} . It can be shown (MERCURE, 2002) that an underestimation of the snowmelt amounts may also lead to too small a_i values. Thus, $1/a_i$ tends to be too large which results in too large values of R_{obs} and consequently in a too small $Bias(R)$, which again leads to too large $Bias(E)$ values. Compared to the uncertainty in the estimate of ΔWS_{obs} , the uncertainty in the estimate of R_{obs} is much smaller.

A rough estimate of how much a more realistic snowmelt in the HIRHAM simulation would have reduced $Bias(E)$ can be obtained from Fig. 15, showing the estimated biases in the hydrological cycle for the HadRM3H model. As indicated in Fig. 7 the snowpack, and thus the snow melting in the melting period, is more realistic in the HadRM3H model simulation, almost as observed (the USAF/ETAC climatological values; Foster and Davy, 1988). Therefore, it seems likely that if we had had a realistic snow pack in the HIRHAM simulation the $Bias(E)$ curve in Fig. 9, in the melting period, would have been lowered approximately by the same amount as the difference between the $Bias(EQ)$ and $Bias(E)$ curves in Fig. 15. This seems not to be sufficient to reduce the HIRHAM $Bias(E)$ to the $Bias(ER)$ values in the melting period, so a realistic snow melt may have influenced also the determination of the a_i which may then have lead to a further reduction of the $Bias(E)$ values in the melting period. On the other hand it should be mentioned that the b_i in Eq. (4) obtained from the HadRM3H model are probably too small due to the fact that almost the whole snowmelt enters the soil so that the change in ΔWS is much smaller than in reality. This may lead to an underestimation of the HadRM3H $Bias(E)$. ERA has the same characteristics with regard to the snowmelt (Hagemann and Dümenil Gates, 2001) which may cause an overestimation of evapotranspiration in the melting period which would yield in an underestimation of $Bias(ER)$.

Thus, as a consequence of the too weak melting in HIRHAM both the ΔWS_{obs} , determined from observed precipitation, and to a lesser extent the R_{obs} determined from observed discharges, are estimated too large. Consequently the estimated $Bias(E)$ determined from Eq. (1) becomes too little. It follows that both the magnitude of $Bias(E)$ and the magnitude of $Bias(C)$ in Fig. 9 are somewhat too large in the months February to May. The almost perfect agreement between $Bias(E)$ and $Bias(ER)$ in the months November to January supports our believe in the realism of both estimates during these months and suggest that the deviations

between the estimates in the rest of the months are explained mainly by the too little snow pack in HIRHAM. Consequently, we consider $Bias(ER)$ and the corresponding $Bias(CR)$ estimates, determined by Eq. (6) in the form

$$Bias(CR) = BiasP - Bias(ER) \quad (8)$$

to be more realistic throughout the year than the $Bias(E)$ and $Bias(C)$ estimates, respectively.

During the spring season, the averaged moisture in the soil of the model is at its maximum value (Fig. 8). At that time at least plenty of soil moisture is available for evapotranspiration. Later, in the summer and autumn seasons, when the averaged model soil moisture is approaching its minimum in September, less and less soil moisture is available for evapotranspiration. The fact that the evapotranspiration bias has a minimum in the autumn, near the minimum of the model soil moisture indicates that the drying is excessive in the model compared to reality. We have no observed soil moisture for validation, but the estimated negative biases of ΔWS in April and May (see Fig. 9) indicate that the drying in the model in spring is in fact excessive. (The same conclusion is reached when considering estimated biases of Fig. 9 with respect to the ERA data). Thus, it seems that in the autumn the bias of evapotranspiration becomes negative, because the evapotranspiration in the model is more restricted by a lack of available soil moisture than it is in reality. Obviously, an excessive drying of the soil in the catchment can also explain the decrease of the excessive divergence of moisture in the late summer and the autumn indicated in Fig. 9 since in that case it is unlikely that even dryer air can be advected into the catchment from the surroundings. As explained below, we think that erroneous advection of excessive dry air from the surroundings explain the periods of excessive divergence of moisture from the catchment, i.e. the periods of the year with negative $Bias(CR)$. After September, the model soil moisture (Fig. 8) begins to rise again, most likely due to increasing precipitation caused by the normal seasonal changes in the general circulation.

Earlier results, *Wild et al.* (1995) making a one-column simulation with the HIRHAM surface scheme driven with observed atmospheric data from the Cabauw site and *Hagemann et al.* (2001) making 3D HIRHAM model experiments testing the sensitivity to changes in prescribed initial (1st July) soil moisture, have indicated that deficiencies in the model representation of the land surface processes cannot be a main reason for the summer drying problem of HIRHAM.

In agreement with that we find here that the increasing negative precipitation bias (in the period May to July) is caused by excessive convergence of dry air which more than compensates a positive bias in evapotranspiration. Therefore, let us at first look for physical reasons for the excessive evapotranspiration simulated by the model during this period (and other periods in the yearly cycle). Obviously, in reality as well as in the model the excessive evapotranspiration may be explained by too high temperatures, and/or too low humidity in the air, and/or too high wind speeds, and/or a too unstable boundary layer in the model. Fig. 3 shows that for HIRHAM the bias of the temperature relative to the CRU data is positive throughout the year, indicating that this is connected to the excessive evapotranspiration. We have not yet examined if other of the factors mentioned above are contributing, However, it seems likely that they are. At least, the too high temperatures are most likely connected with reduced vertical stability in the boundary layer and with reduced relative humidity, which is further reduced by the inflow of dry air from the surroundings.

The reduced evapotranspiration bias in the spring, indicated by the $Bias(ER)$ estimate, in spite of a too high averaged temperature over the whole catchment, may be explained by the fact that where the melting occurs and part of the evapotranspiration takes place the soil temperature in both the model and in ERA is 0 °C, and thus here, to the extent that these areas are common, it is neither too warm nor too cold in the model compared to ERA. The averaged ERA catchment temperature is too cold in winter and neighbour seasons, as seen in Fig. 3, and thus the $Bias(ER)$ estimates tend to be too small. However, at low temperatures the evapotranspiration is not so sensitive to the precise value of the temperature. But it could imply that the true evapotranspiration values are somewhat higher than $Bias(ER)$.

From Fig. 10, which shows the deviations of the HIRHAM surface energy fluxes from ERA, it seems obvious that the reason for the too high temperature is an excessive solar radiation. Considering the fact that the ECHAM4 short wave radiation scheme, which is used in HIRHAM, has been validated to behave realistically (*Wild et al.*, 1996), it seems most likely that the reason for the excessive solar radiation is a too small cloud cover. Note that the times of the maximum bias in solar radiation and in temperature are in agreement with this explanation, the former in August and the latter delayed to between August and September. We have not yet been able to validate this explanation directly against data, i.e. to show that the model has a negative bias in cloud cover.

With the main purpose to understand the excessive divergence of moisture indicated in Fig. 9 we studied monthly values of the systematic mean sea level pressure (MSLP) errors, i.e. the deviation between the HIRHAM simulation and the ERA data. These bias maps are discussed extensively in *MERCURE* (2002). Here we shall just consider the effects of the general mean circulation biases, which are implied by these pressure biases. These circulation biases can be decomposed into geostrophic and a-geostrophic components. Let us consider at first the biases in the a-geostrophic flow. Note at first that in an area of positive MSLP bias there will be excessive upper level horizontal convergence, excessive vertical subsidence and excessive low level horizontal divergence. In areas of a negative MSLP bias, on the other hand, there will be excessive low level convergence, excessive up lift with enhanced precipitation and excessive upper level divergence. In the areas of positive MSLP bias, at low levels, the excessive subsidence will create too low humidity, and there will be an erroneous low level mean flow of too dry air toward the areas of too low pressure. As this flow approaches the areas of too low pressure it picks up moisture by evapotranspiration from the surface and from precipitation so that a moisture gradient builds up. Thus, everywhere except near the centres of the areas of positive MSLP biases, there will be an erroneous mean flow advection at low levels of too dry air, or equivalently an excessive divergence of moisture. Outside the areas of too high pressure, the mean a-geostrophic component of the bias at high levels is generally less important as there the moisture content in the air is relatively small. In the areas of too high pressure the humidity tends to be the same at low and high levels and therefore here the convergence of moisture at high levels tends to balance the divergence of moisture at low levels.

An inspection of the monthly MSLP bias maps (not shown) reveals that, except in August and September, the Danube catchment is situated in areas of negative MSLP bias or in the boundary zone between negative and positive biases. Thus, generally, the biases in the mean a-geostrophic flow should imply an excessive divergence of moisture from the catchment which is largely in agreement with Fig. 9. An exception is the period February to April where the $Bias(ER)$ values are near zero. Apart from the fact that $Bias(ER)$ tends to be underestimated in the winter and spring, this may be explained by the relatively homogeneous monthly MSLP bias fields over the Danube catchment in these months. In August and September the

catchment is situated inside positive MSLP bias areas and thus the net transport of moisture by the mean a-geostrophic error flow at high and low levels should balance, approximately. This is again in agreement with the *Bias(CR)* estimate in Fig. 9, which is indicating a reduction to small positive biases of moisture divergence in these months. Thus we find that the systematic errors in the a-geostrophic mean flow seem to explain the erroneous moisture divergence out of the Danube catchment throughout the year as indicated in Fig. 9. Throughout the year the advection of moisture by the geostrophic component of the flow bias do not seem to be of any importance. It should be mentioned that also biases in eddy moisture transports may have contributed to the erroneous moisture divergence, indicated in Fig. 9, although such biases have not been considered here.

Summary

Throughout the year the solar radiation at the surface in the HIRHAM simulation is estimated to be excessive, probably because of too little clouds simulated. This leads to too high surface air temperatures and probably a too unstable boundary layer, which both lead to excessive evapotranspiration as long as sufficient soil moisture is available. The too high temperatures in winter may, at least partly, explain also the too small snow pack simulated. During spring small temperature biases over areas of snow melt seem to explain the estimated small evapotranspiration biases in that season. Due to compensating excessive divergence of moisture, apparently caused by systematic errors in the general a-geostrophic circulation of the atmosphere, the excessive evapotranspiration is not returned to the soil in the catchment in the form of a similar amount of excessive precipitation. On the contrary, the divergence of moisture seems to dominate during the months May to July which leads to negative precipitation biases in the summer and autumn seasons. This and the excessive evapotranspiration contribute to an excessive drying of the model soil, which is becoming so dry that the evapotranspiration bias turns negative in August and September, in spite of too high surface air temperatures. The long term balance of soil moisture is maintained by a negative bias in runoff throughout the year. Thus, in the model the catchment as a whole loses an excessive amount of moisture through its lateral boundaries in the atmosphere, but saves a similar amount of moisture by too little integrated runoff, or in other words by too little discharge from the catchment.

We conclude that, as the reason for the too large solar radiation at the surface seems to be systematically, too little cloud cover is probably caused by an error in the parameterization which should be investigated. Further, it should be investigated if there are other reasons than those suggested here for the periods of excessive evapotranspiration. Also the reason(s) for too little snow pack other than the excessive temperature should be located. The fact that the HadRM3H model simulation has almost the right snow pack, in spite of winter temperatures approximately similar to those in the HIRHAM simulation, indicates that the insufficient snow pack is not caused by too smooth mountains in HIRHAM as it has been suggested previously for Scandinavia (*Christensen et al.*, 1998).

4.2.2. ARPEGE

ARPEGE simulates too much convergence in the winter (see Fig. 11) which is consistent with the overestimated precipitation and the accumulated snowpack. In the spring, too little convergence is simulated. It seems that the convergence of moisture into the catchment is weakened due to too much moisture in the atmosphere which may partly be caused by the overestimated evapotranspiration. As there is also too little upward surface solar radiation compared to ERA data (see Fig. 12), this may indicate too much simulated cloud cover in the

spring. In principle, too little upward surface solar radiation may also be caused by a too low albedo. But the largely overestimated snow cover would rather imply a too large albedo. Moreover the overestimated snow cover seems to cause an underestimation of the upward (negative) sensible heat flux at the same time.

4.2.3. CHRM

During the summer the large negative bias in precipitation (Fig. 13) is almost compensated by the bias in evapotranspiration so that the bias in convergence is small. This indicates that the summer drying problem is not related to the atmospheric transport of moisture into the area. The too little upward latent heat flux compared to ERA (see Fig. 14) corresponds well with the underestimated evapotranspiration in the summer. Since the 2m temperatures are too cold throughout the year except during the summer (cf. Fig. 3) it was initially thought that this may be related to a too large albedo (see below). In the summer, the effect that causes the too cold temperatures seems to be compensated by too little cloud cover as indicated by too large surface solar radiation accompanied by too large upwards sensible heat flux and surface thermal radiation. The underestimation of cloud cover is presumably induced by the underestimated evapotranspiration that provides the atmosphere with too little moisture.

The surface albedo (not shown), when compared to ERA fields, shows very good agreement for snow-free values, while retaining a good yearly cycle connected to the snow cover. Experiments with the relationship between the snow amount, the snow cover and the total surface albedo have resulted in very small sensitivities. Since the snow amount, snow melt and runoff all seem quite correct, surface albedo does not seem to hold the explanation for the surface radiative balance problem.

During the early spring, a lessening of the surface solar deficit is shown (Fig. 14), which has been however partitioned into producing a slightly larger peak of summer (about 15 W/m^2) positive solar bias which seems to cause a slightly larger sensible heat bias and corresponding slightly more negative latent heat (more than 20 W/m^2) and positive thermal radiation biases. Therefore it is plausible that errors in the soil-vegetation-atmosphere transfer scheme (SVATS) could be the cause for the local tendency of the model to become dry and warm over summer, since the energy lost in sensible heat and thermal radiation should and could be used for evapotranspiration. The biases in precipitation and their explanation (see above) agree with this.

In the winter the error in the 2m temperature (cf. Fig. 3) seems to track the signal in the ERA-15 data but is certainly smaller (-3 to -2 K versus -4 K). This may indicate a connection with a signal from the driving data travelling through the model domain from the lateral boundaries. But this explanation should be more valid for grid points near the domain boundaries. A simulation for one season with altered near-surface lateral boundary conditions does not show a large impact on the simulated temperatures.

An analysis of the daily minimum and maximum 2m temperatures over Europe has shown that the minimum temperatures are simulated too high and the maximum temperatures are simulated too low, especially in the South. This is induced by the force restore soil model which uses a 1-year time scale bottom boundary condition that constrains the surface temperature oscillation. Therefore the diurnal cycle is dampened, and it might be that the diurnal cycle is also shifted in time as the time constant of 1 year introduces a phase error in the top (thin) layer of soil which should represent the diurnal oscillation. *Jacobsen and Heise*

(1982) have shown that the phase error can be as large as 50% on the limb of the two periods represented by the time constants in the model (1day, 1 year) and that the time shift can be of several hours. This will be further examined in studies that are planned with a multi-layer soil model.

4.2.4. HadRM3H

Considering the quasi-observed evapotranspiration obtained from the HadRM3H simulation, the dry bias in precipitation (Fig. 15) is almost compensated by the bias in evapotranspiration which yields no significant bias in convergence. But if EQ_{obs} obtained from the HIRHAM simulation is considered, a positive convergence bias in the summer and a negative convergence bias in the spring can be seen. The underestimation of the upward latent heat flux compared to ERA (Fig. 16) corresponds to values that lie in between the two evapotranspiration biases. This demonstrates the large uncertainty in the estimate of the observed evapotranspiration. At the same time, the upward sensible heat flux and the upward surface thermal radiation are largely overestimated as well as the downward surface solar radiation which is too large throughout the year. Thus, there is too much absorption of energy in the soil which causes the severe warm bias (Fig. 3) and which is a clear indicator for a too low albedo. The low albedo is directly connected to a lack of clouds which itself is induced by the fact that too little moisture is advected into the region as indicated by the negative convergence bias CQ_{obs} in the spring (Fig. 15).

The above implies that the overestimate of precipitation seen in the first two months of spring results from too high evaporation and thus the convergence bias (from the definition in Eq. (6)) then is negative. The precipitation bias then changes sign in May whilst the evaporation bias is still positive and thus the convergence bias becomes even more negative. This implies that there is a strong circulation component in the cause of the dry bias in May and suggests that this is the underlying cause of the subsequent warm and dry bias throughout summer. The lack of convergence restricts precipitation and associated clouds which thus (further) increases the short wave radiation and surface heating/temperature. The evaporation is then able to balance most of this heating in May but this depletes soil moisture sufficiently to limit this mechanism, and also evaporation to maintain the hydrological cycle, throughout summer. This mechanism is confirmed in the more detailed analysis of Jones *et al.* (2002).

4.2.5. REMO

REMO shows large negative biases in precipitation and evapotranspiration ranging from the late spring to the autumn (Fig. 17). The large underestimation of the summer evapotranspiration is directly related to the overestimation of the 2m temperature (see Fig. 3). The first intensifies the dry bias in precipitation and the latter causes the too large negative upward flux of surface thermal radiation (Fig. 18). The warm temperature bias is caused by insufficient convective activity, which leads to a too small amount of clouds and precipitation in the summer, thereby allowing a too strong radiative heating of the surface indicated by too large downward surface solar radiation and too large upward sensible heat flux in the summer.

As REMO has somewhat less evapotranspiration than HIRHAM in the spring, the soil is slightly moister and, in principle, about the same amount or even more water is available for evapotranspiration in the summer. But the fact that the REMO summer evapotranspiration is much less than in HIRHAM may suggest that the advection of dry air and such the divergence of moisture out of the Danube catchment is considerably smaller than in HIRHAM. A detailed investigation of the mean atmospheric circulation is under preparation.

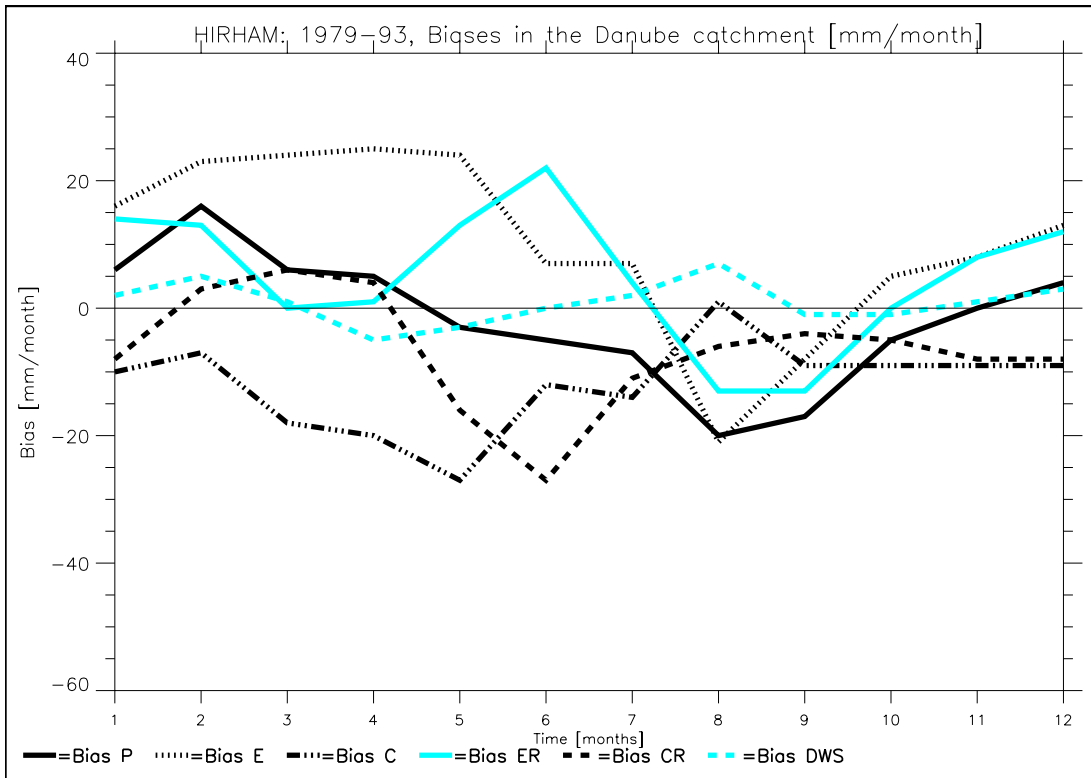


Fig. 9. Biases in the hydrological cycle of the HIRHAM simulation (1979-93) in mm/month over the Danube catchment. P = precipitation, E = evapotranspiration, C = convergence, ER = evapotranspiration (using ERA data), CR = convergence (using ER), DWS = Storage change = ΔWS

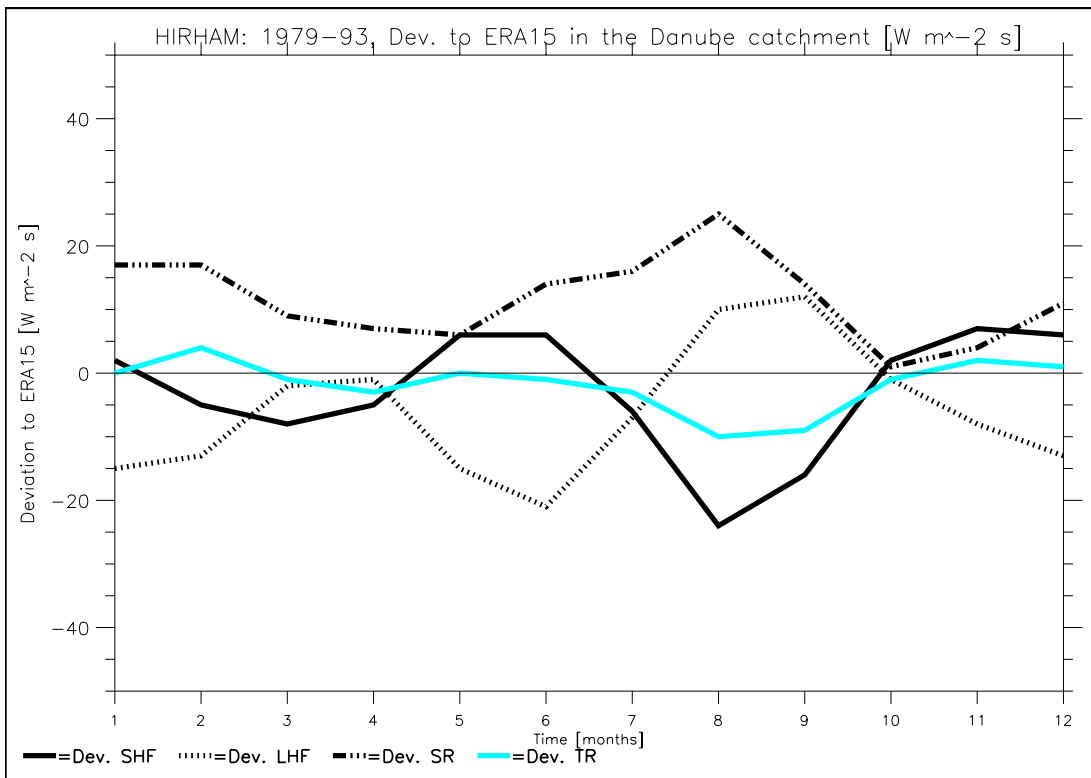


Fig. 10. Deviations from ERA of the surface energy fluxes of the HIRHAM simulation (1979-93) in $W m^{-2} s$ over the Danube catchment

SHF = sensible heat flux, LHF = latent heat flux, SR = surface solar radiation, TR = surface thermal radiation

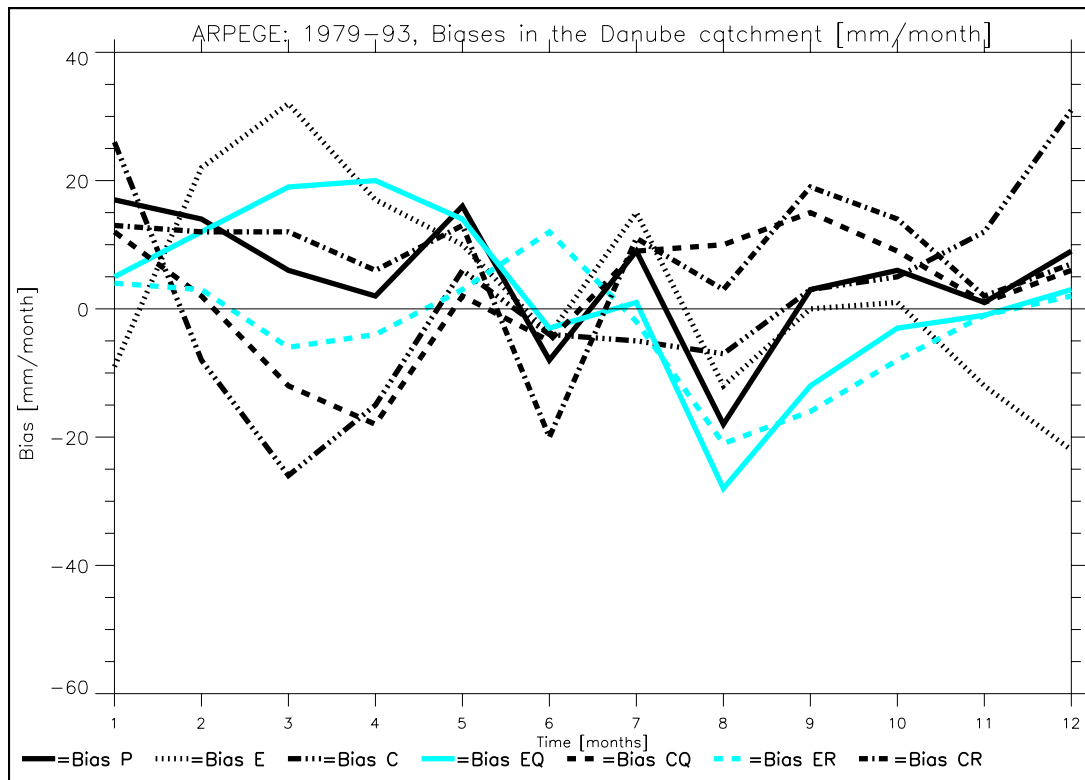


Fig. 11. Biases in the hydrological cycle of the ARPEGE simulation (1979-93) in mm/month over the Danube catchment. P = precipitation, E = evapotranspiration, C = convergence, EQ = evapotranspiration (2nd estimate), CQ = convergence (using EQ), ER = evapotranspiration (using ERA data), CR = convergence (using ER)

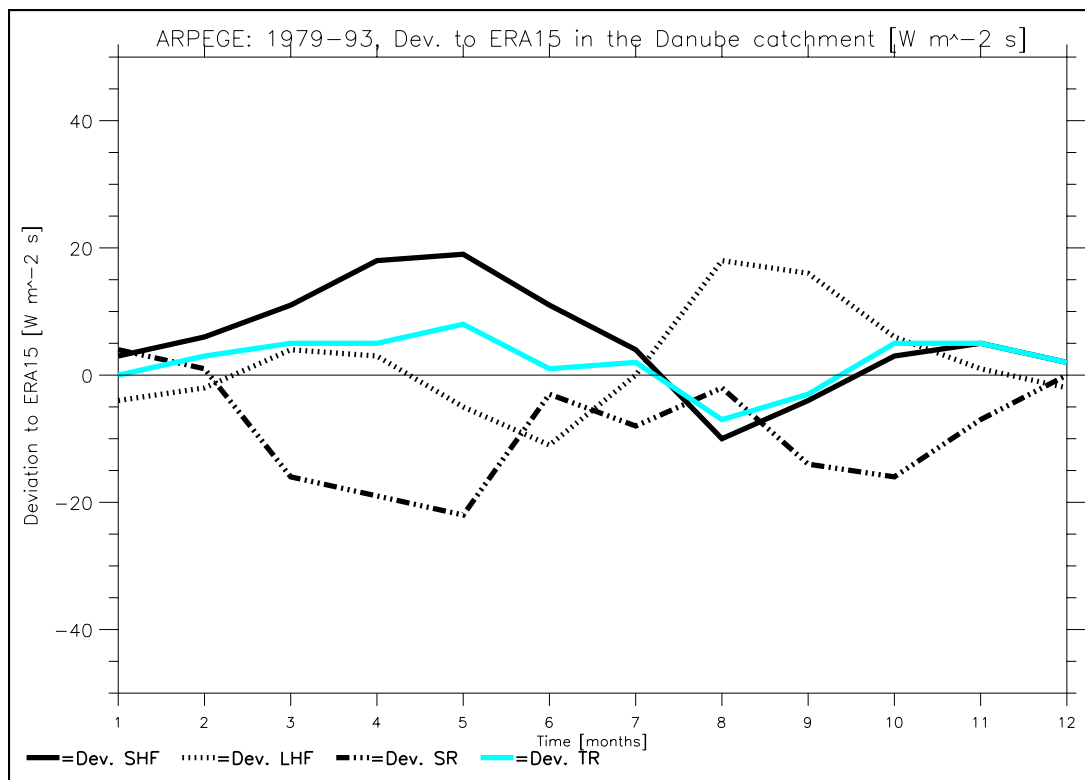


Fig. 12. Deviations from ERA of the surface energy fluxes of the ARPEGE simulation (1979-93) in Wm⁻²s over the Danube catchment
SHF = sensible heat flux, LHF = latent heat flux, SR = surface solar radiation, TR = surface thermal radiation

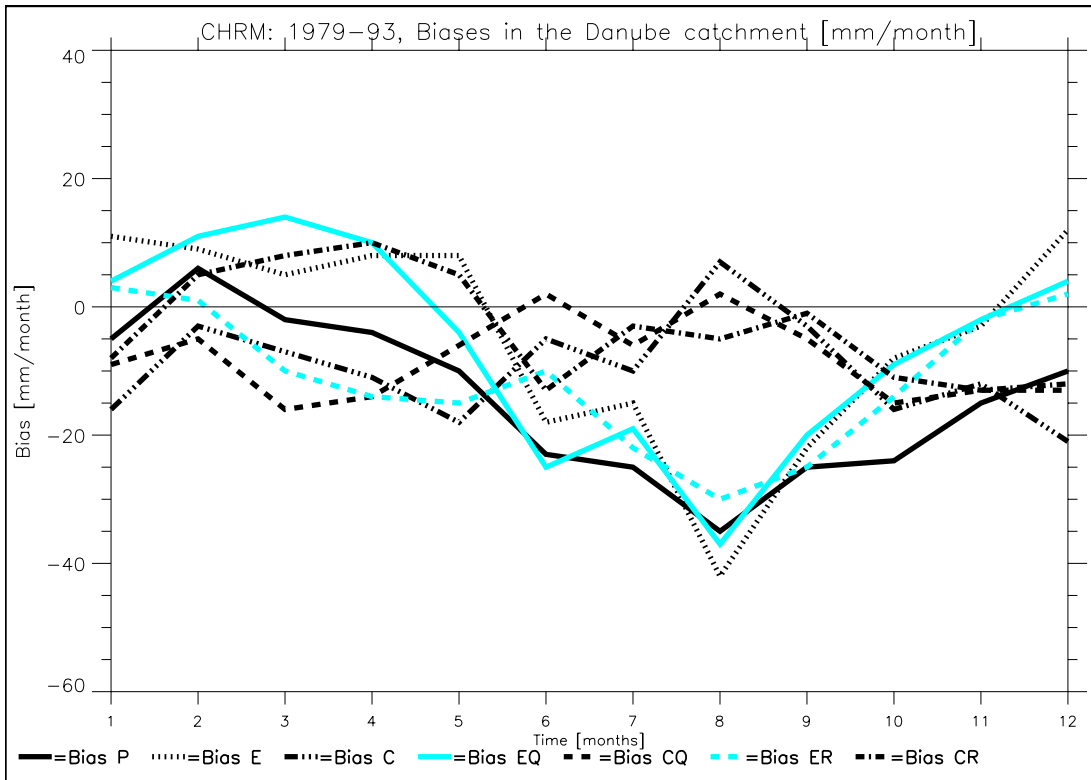


Fig. 13. Biases in the hydrological cycle of the CHRM simulation (1979-93) in mm/month over the Danube catchment. P = precipitation, E = evapotranspiration, C = convergence, EQ = evapotranspiration (2nd estimate), CQ = convergence (2nd estimate), ER = evapotranspiration (using ERA data), CR = convergence (using ER)

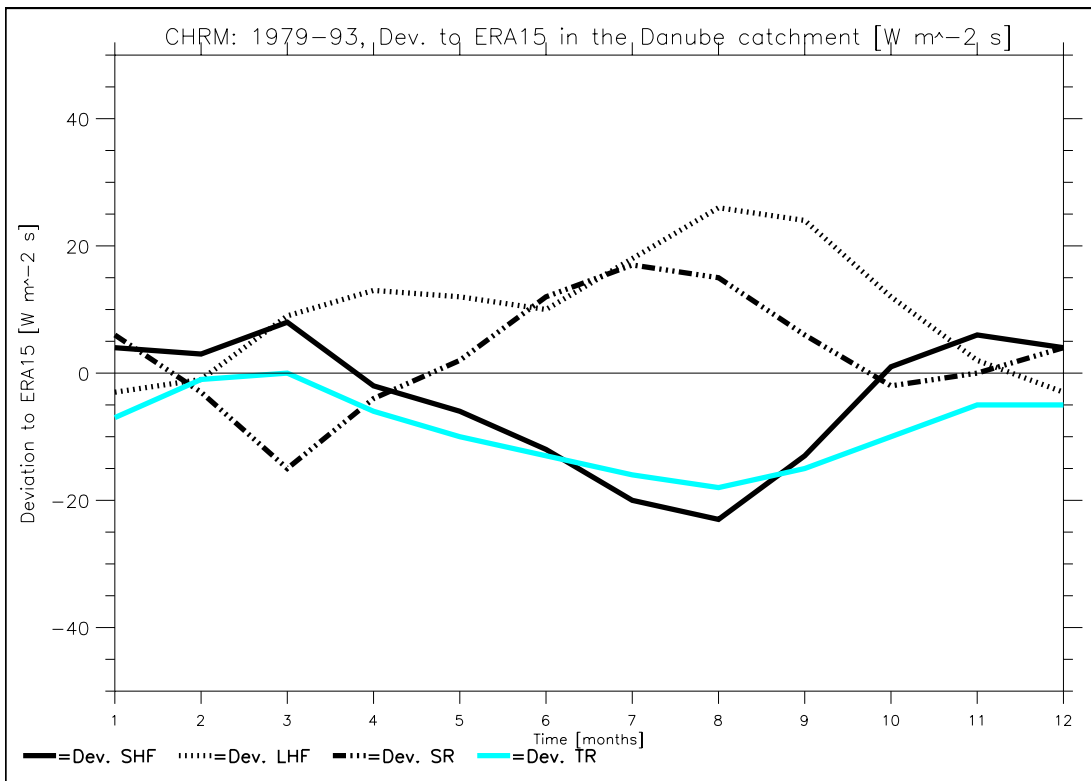


Fig. 14. Deviations from ERA of the surface energy fluxes of the CHRM simulation (1979-93) in Wm⁻²s over the Danube catchment
SHF = sensible heat flux, LHF = latent heat flux, SR = surface solar radiation, TR = surface thermal radiation

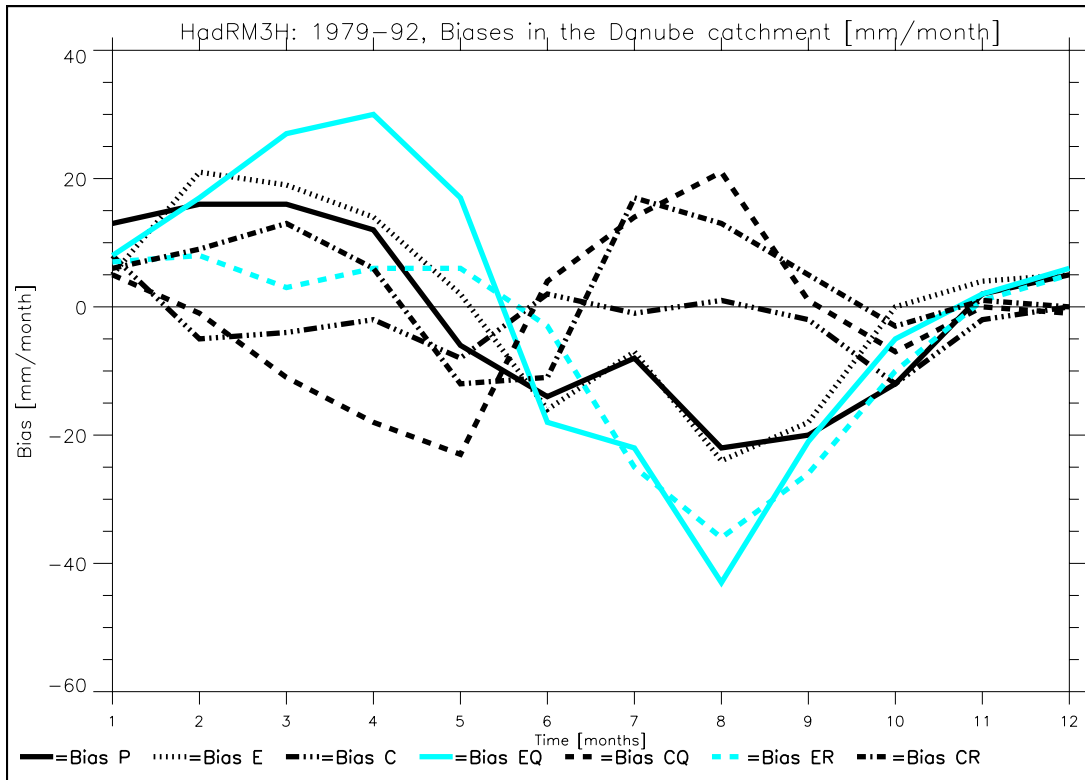


Fig. 15. Biases in the hydrological cycle of the HadRM3H simulation (1979-92) in mm/month over the Danube catchment. P = precipitation, E = evapotranspiration, C = convergence, EQ = evapotranspiration (2nd estimate), CQ = convergence (2nd estimate), ER = evapotranspiration (using ERA data), CR = convergence (using ER)

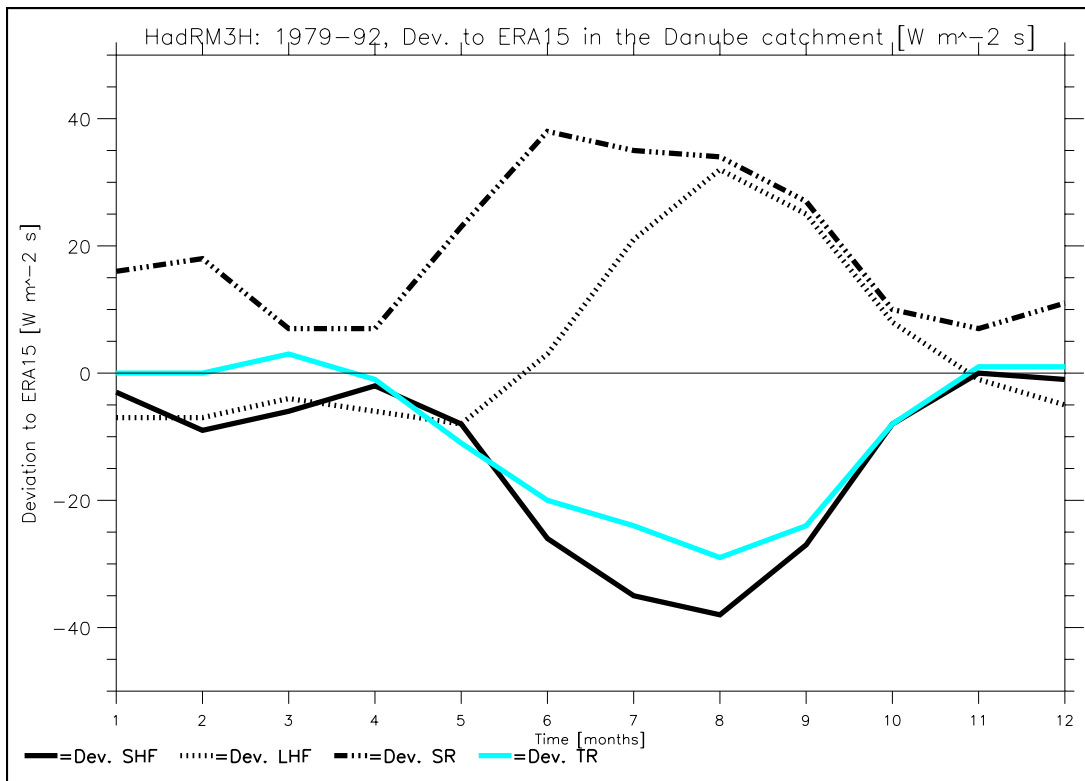


Fig. 16. Deviations from ERA of the surface energy fluxes of the HadRM3H simulation (1979-92) in Wm⁻²s over the Danube catchment
 SHF = sensible heat flux, LHF = latent heat flux, SR = surface solar radiation, TR = surface thermal radiation

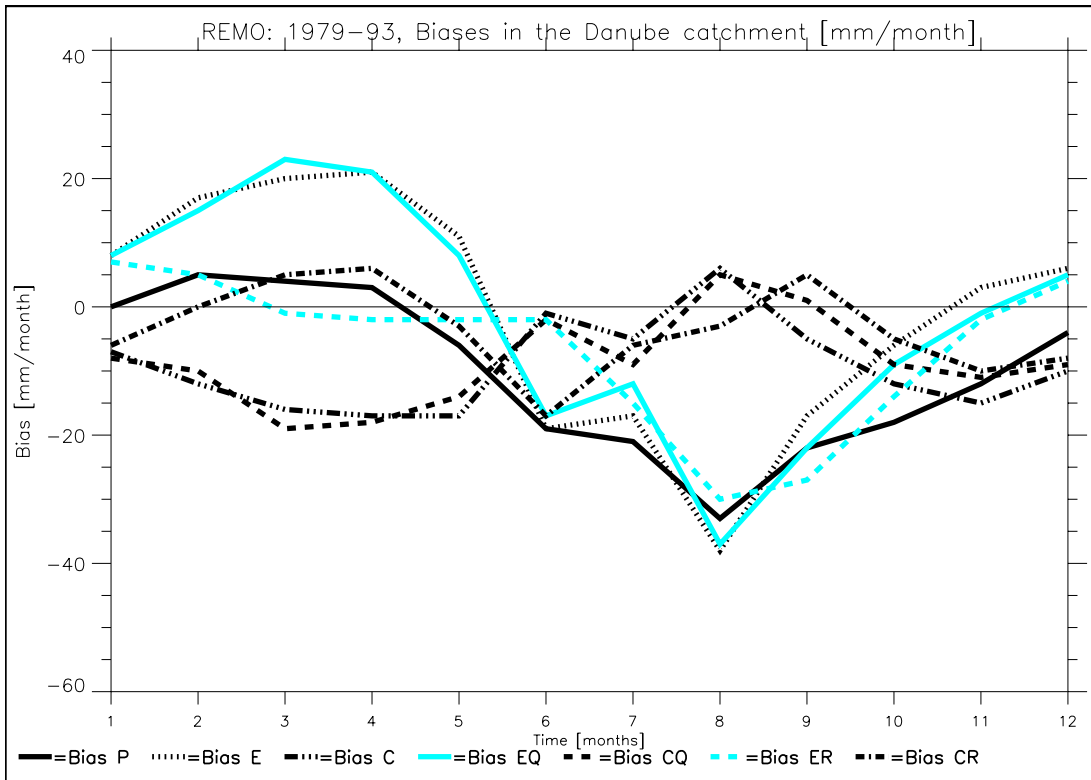


Fig. 17. Biases in the hydrological cycle of the REMO simulation (1979-93) in mm/month over the Danube catchment. P = precipitation, E = evapotranspiration, C = convergence, EQ = evapotranspiration (2nd estimate), CQ = convergence (2nd estimate), ER = evapotranspiration (using ERA data), CR = convergence (using ER)

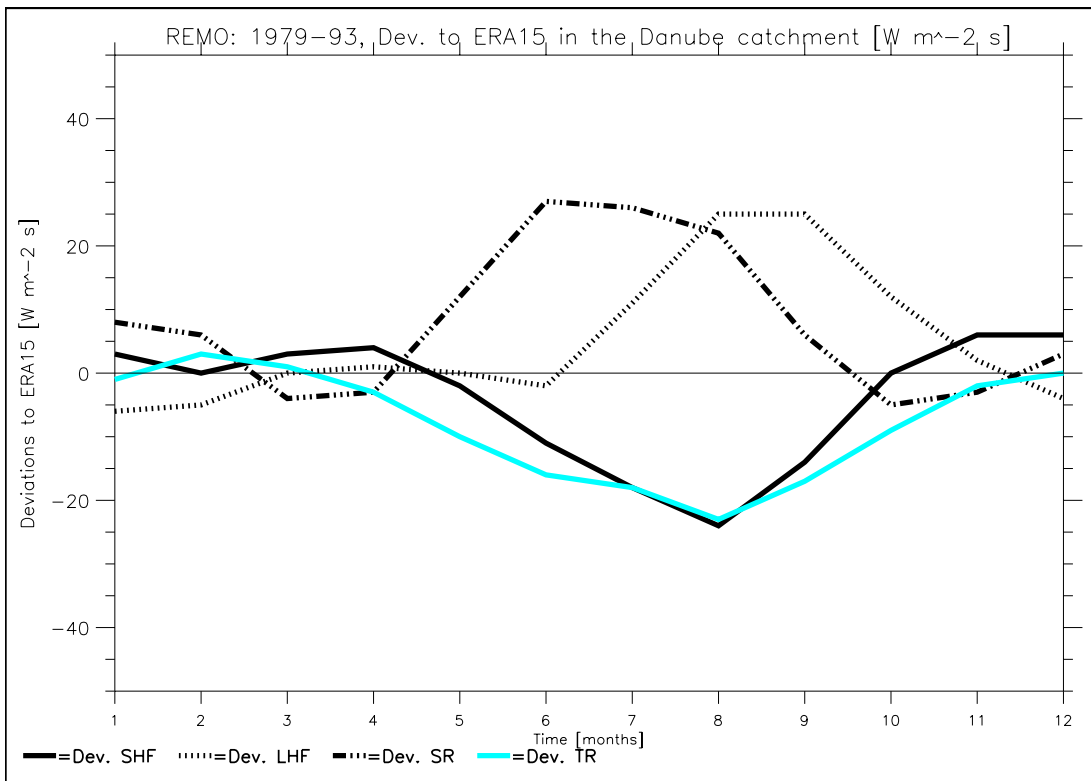


Fig. 18. Deviations from ERA of the surface energy fluxes of the REMO simulation (1979-93) in $W m^{-2} s$ over the Danube catchment

SHF = sensible heat flux, LHF = latent heat flux, SR = surface solar radiation, TR = surface thermal radiation

5. The Baltic Sea catchment

The location of the Baltic Sea catchment is shown in Fig. 1. Its area comprises about 1729000 km² and the annual mean discharge into the Baltic Sea is about 15323 m³/s (483 km³/a). As in Sect. 4, all atmospheric variables were integrated over the whole catchment area and the water fluxes will be expressed in mm/month instead of a volume flux unit. In Sect. 5.1, the different simulated variables of all models are directly compared to each other and to observations. The results of this section are summarized in Table 2. The biases in the water balances and the deviations from ERA data in the energy balance are analysed for each model separately in Sect. 5.2.

Table 2. Overview over regional climate model performance in the Baltic Sea catchment.

‘+’ designates overestimation, ‘-’ underestimation, ‘o’ good simulation, and ‘.’ no clear rating possible.

Simulated value		HIRHAM	ARPEGE	CHRM	HadRM3H	REMO
2m temperature	winter	o	o	-	o	-
	spring	o	--	-	o	-
	summer	o	o	o	o	+
	autumn	o	-	-	o	o
Precipitation	winter	+	+	+	+	+
	spring	+	+	+	+	+
	summer	o	o	+	o	o
	autumn	+	+	o	+	+
Evaporation	winter	+	o	o	o	o
	spring	+
	summer
	autumn
Total Runoff	winter	-	-	o	o	o
	spring	-	++	o	-	o
	summer	-	o	o	+	o
	autumn	-	o	o	o	o
Snowpack	winter	-	+	o	o	o
	spring	-	+	o	o	o
	summer	o	o	o	+	o

5.1. Intercomparison between the models

For all models, the comparison of simulated precipitation to CRU observations (Fig. 19) shows the common atmospheric model feature of the overestimation of precipitation over the Baltic sea catchment from the autumn to the spring. This may in part be related to systematic errors in the mean sea level pressure fields that correspond to errors in the near surface general circulation (*Machenhauer et al.*, 1996, 1998) but given that quasi-observed boundary conditions are being used implies a positive bias due to errors in the model physics. In the summer, all models simulate realistic precipitation amounts although they simulate the precipitation maximum in July instead of August. All models except ARPEGE capture the time of the minimum precipitation in February. It has to be mentioned that precipitation measurements in high latitudes tend to underestimate the snowfall amounts. Thus, precipitation data (1981-93) from the BALTEX database (*BHDC*, *SMHI*, personal communication, 2001) are also given in Fig. 19 which are in a very good agreement with the CRU precipitation data and indicate the model biases are real.

Fig. 20 shows that the difference of the simulated 2m temperature and CRU data is small throughout the year for HIRHAM and HadRM3H. The CHRM 2m temperature is generally too cold with a maximum bias in the spring, and it seems that the CHRM temperature bias tracks the ERA data very closely in the winter and early spring. ARPEGE has cold biases in the spring and the autumn which are similar to the ARPEGE biases over the Danube catchment (see Sect. 4.1). REMO seems to have a too enhanced annual cycle in the 2m temperature as it has a cold bias in the winter and early spring, and a warm bias in the summer.

With regard to evapotranspiration (Fig. 21), all models tend to overestimate the evapotranspiration throughout the year except during the summer which is similar to the simulated precipitation bias. In the summer, all models seem to have reasonable evapotranspiration amounts. The comparison of the evapotranspiration and the latent heat fluxes to ERA data (Fig. 22) does not directly correspond to these results, which indicates the large uncertainty in the observed evapotranspiration estimates.

Fig. 23 shows the simulated total runoff compared to the quasi-observed runoff obtained from the HIRHAM simulation. The results of this comparison are quite similar to the results obtained for the Danube catchment (see Sect. 4). This indicates that HIRHAM has a general tendency to underestimate runoff as well as the accumulated snowpack (Fig. 24), while ARPEGE largely overestimates the accumulated snowpack which results in an largely overestimated snowmelt induced runoff peak in the spring and in a delay of this peak. This delay is also connected to the too cold 2m temperatures in spring (see Fig. 20). For HadRM3H, the fact that there is almost no surface runoff generally smoothes the total runoff curve and, thus, the soil is filled by the snowmelt (see Fig. 25) and the runoff peak seems to be caused by rain falling on the full soil moisture reservoirs. REMO and CHRM simulate the runoff very well even though they underestimate the runoff during the autumn. Again, CHRM, REMO and HIRHAM capture the time of the runoff peak in April and all models tend to underestimate the total runoff in the winter which may be related to the overestimated evapotranspiration at the same time. The good simulation of the spring runoff peak of CHRM and REMO is consistent with their simulation of the accumulated snowpack (Fig. 24) during the spring. HadRM3H shows the strange characteristic that it has snow throughout the year within the catchment. These amounts of snow are simulated in several grid boxes in the mountains of Norway where the summer snowpack reaches up to 5 m in one gridbox, which is unrealistic.

All models except for ARPEGE show an increase in soil moisture (Fig. 25) from autumn to the winter. The ARPEGE soil moisture decreases although its precipitation increases at the same time. This indicates that the precipitation falls as snow instead of rain (as it should) which corresponds to the overestimation of the snowpack. As mentioned before, the HadRM3H snowmelt fills the soil in the spring thereby increasing the soil moisture much more than the other models (except for ARPEGE).

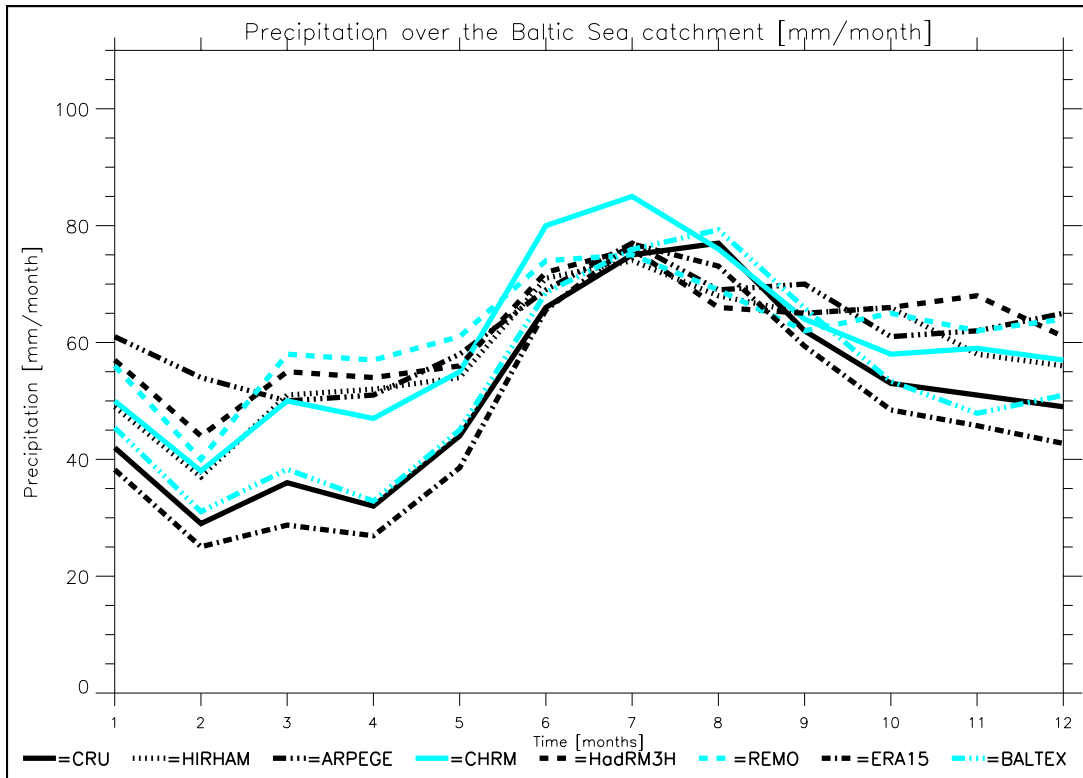


Fig. 19. Precipitation over the Baltic Sea catchment in mm/month

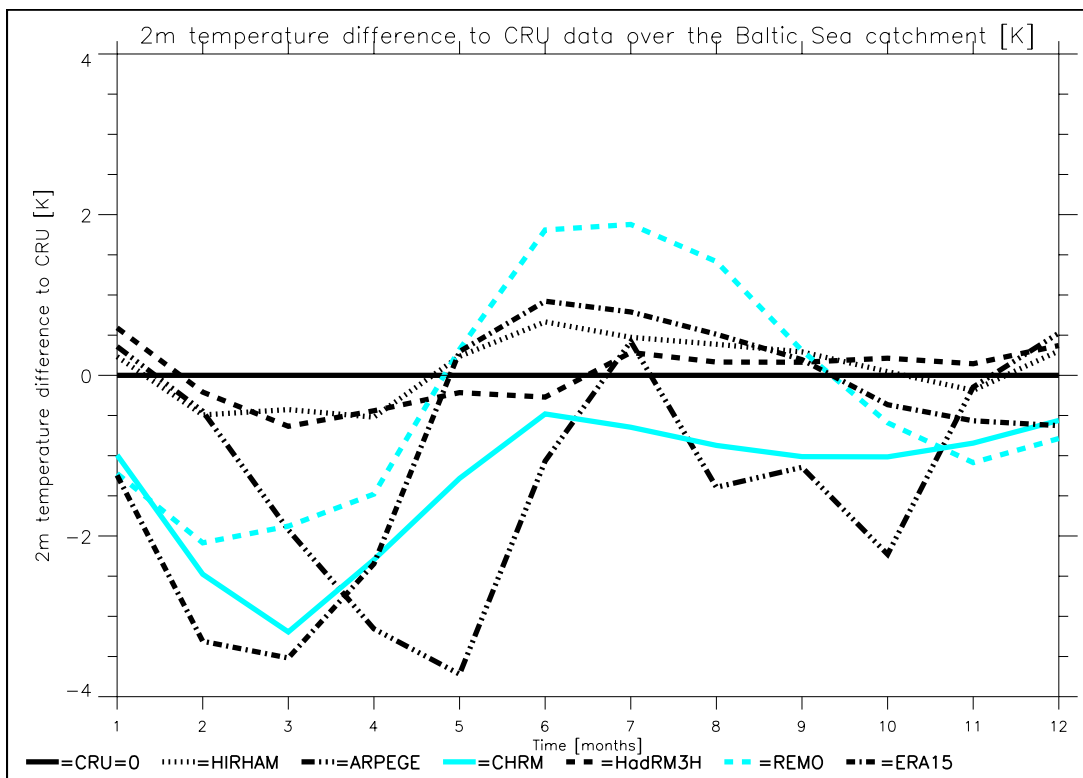


Fig. 20. 2m temperature difference to CRU data over the Baltic Sea catchment in K

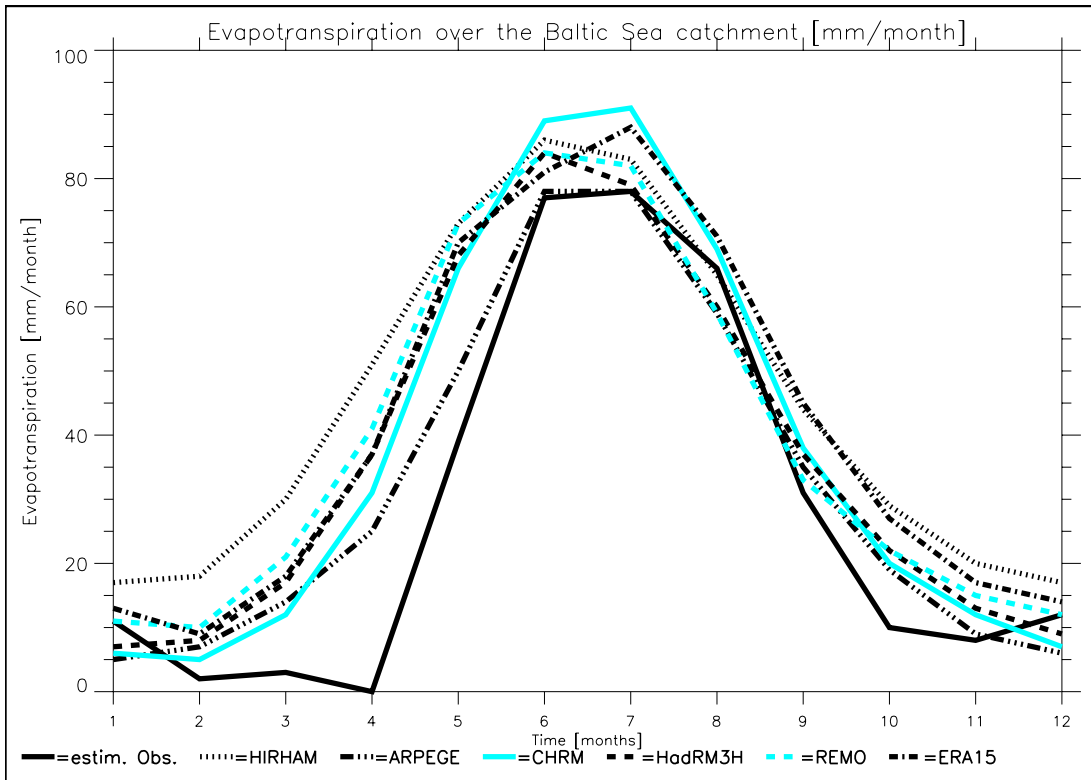


Fig. 21. Evapotranspiration over the Baltic Sea catchment in mm/month

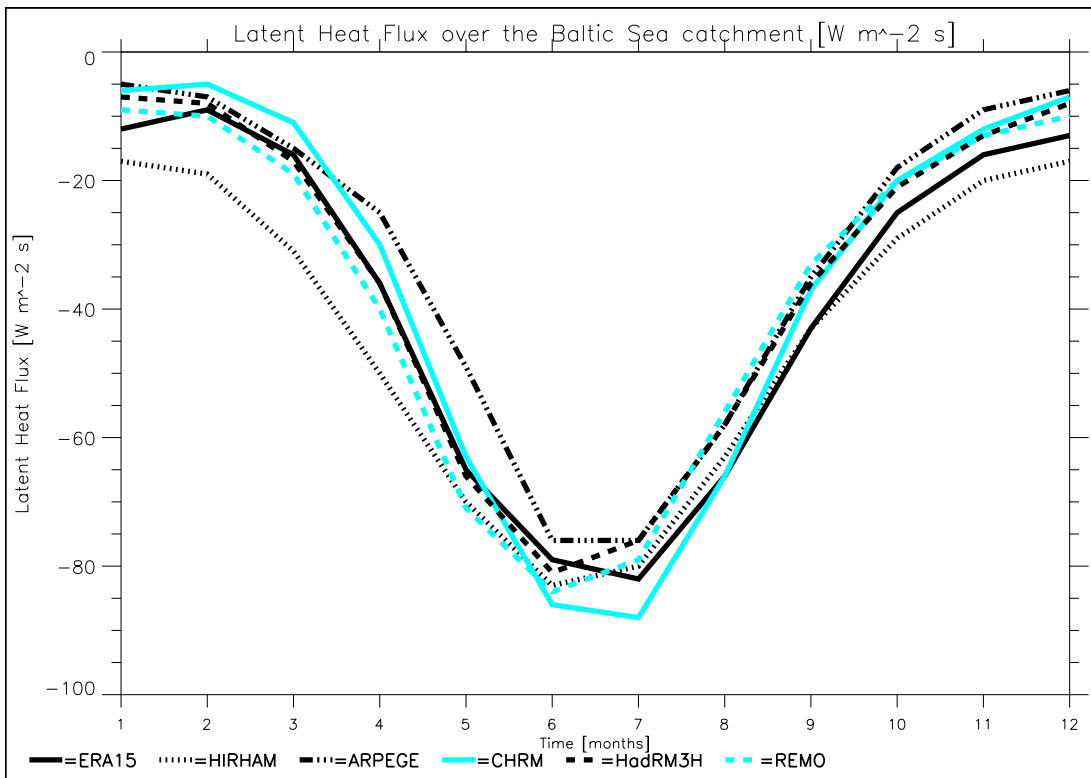


Fig. 22. Latent heat flux over the Baltic Sea catchment in $W m^{-2} s$

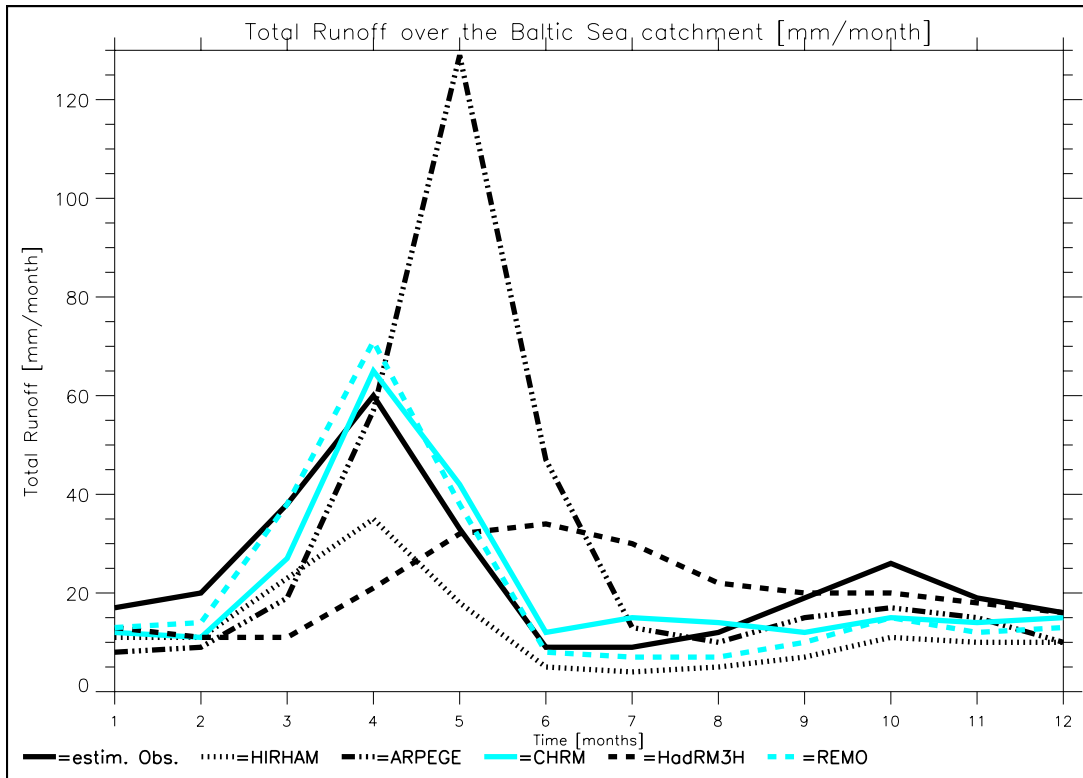


Fig. 23. Total runoff over the Baltic Sea catchment in mm/month

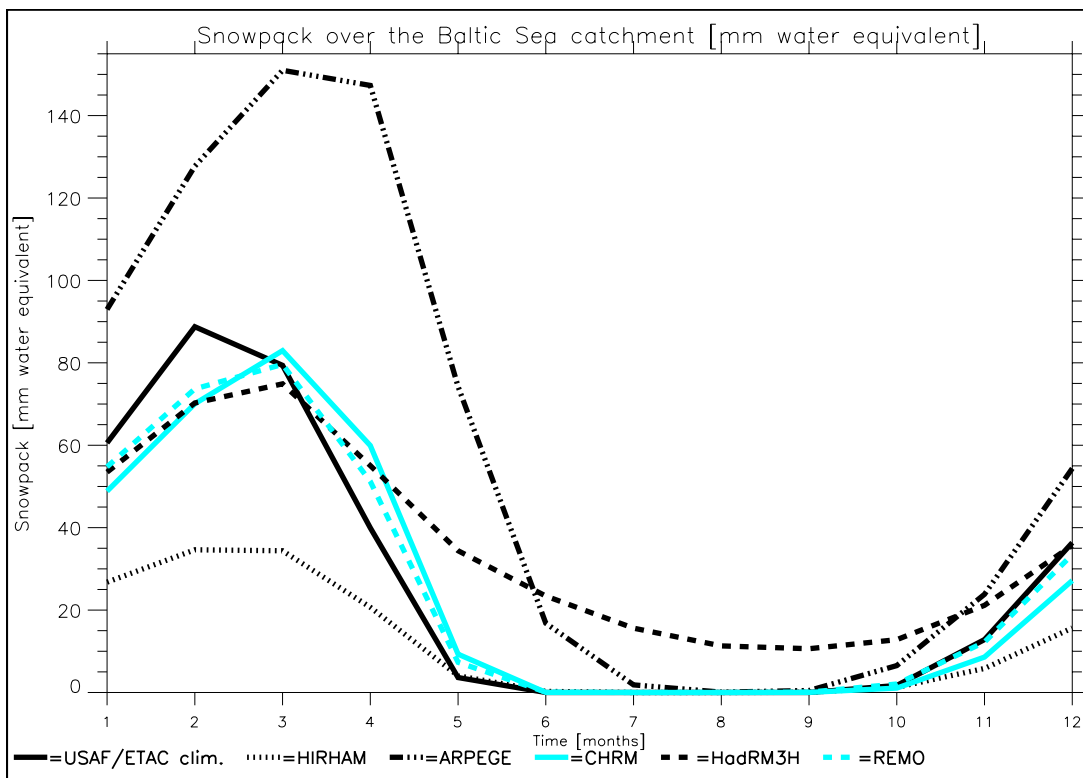


Fig. 24. Mean snow pack over the Baltic Sea catchment in mm water equivalent. USAF/ETAC climatological values of Foster and Davy (1988) are used as observed values for comparison.

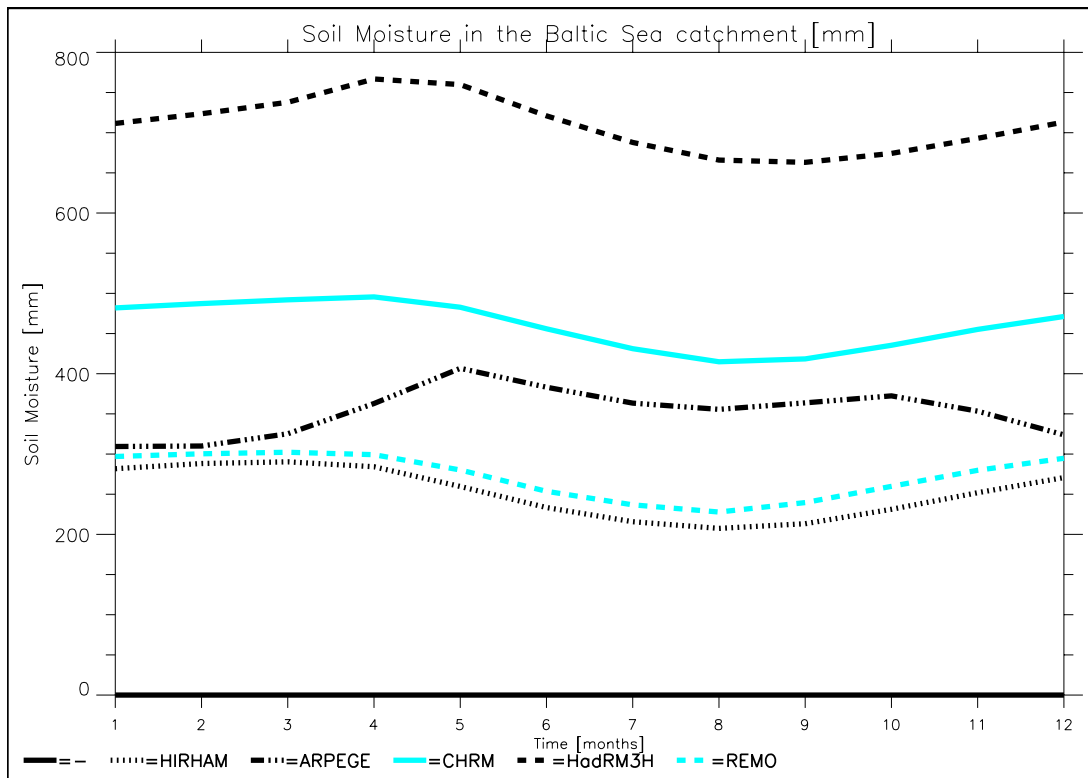


Fig. 25. Mean soil moisture in the Baltic Sea catchment in mm

5.2. Water and energy balances

5.2.1. HIRHAM

Fig. 26 shows the biases in the hydrological cycle for the HIRHAM simulation. Too much precipitation and too much evapotranspiration are simulated in the whole year except during the summer. While the evapotranspiration $Bias(ER)$ using ERA data is close to the precipitation bias, the estimated positive evapotranspiration $Bias(E)$ largely exceeds the precipitation bias. As HIRHAM simulates too little runoff (Fig. 23), $Bias(E)$ seems to be more accurate than $Bias(ER)$ which implies that there is also too much divergence of moisture in the atmosphere, especially in the spring. This suggests that there is too much moisture in the atmosphere which is partially caused by the overestimated evapotranspiration. This is consistent with the deviation of the simulated latent heat flux (negative upward) from the ERA data (Fig. 27). The too large upward surface thermal radiation in the winter and the spring seems to be related to the underestimated snow cover, which probably also causes a too low albedo as indicated by an overestimated surface solar radiation in the winter. Since this is compensated by an overestimation in the latent heat flux, the 2m temperatures are simulated well. The too little surface solar radiation in the summer is partially compensated by too little upward sensible heat flux at the same time.

5.2.2. ARPEGE

The biases in the hydrological cycle of the ARPEGE simulation are shown in Fig. 28. The overestimation of evapotranspiration in the spring (March/April) seems to moisten the atmosphere too much so that there is too little convergence of moisture from other regions. As

stated before (Sect. 5.1) the large runoff bias in the spring is related to the overestimated snowpack.

The deviations of the surface energy fluxes from ERA data (Fig. 29) reveal that the downward surface solar radiation is far too low from April to September which seems to be related to a too large background albedo. This is supported by the fact that this deviation is close to zero when snow is covering the surface during the winter. A too low cloud cover seems not to be responsible for this deviation since precipitation is simulated quite well at the same time. The underestimated heating by the too low surface solar radiation also causes the cold biases in the spring and the fall. Only in the July this does seem to be compensated by other effects.

5.2.3. CHRM

For CHRM, the positive precipitation bias (see Fig. 30) is almost compensated by the positive evapotranspiration bias except in the spring when the latter is much larger. The overestimated evapotranspiration seems to moisten the atmosphere too much thereby causing too little convergence into the catchment area. CHRM simulates too little surface solar radiation compared to ERA (Fig. 31) at the same time. This underestimation may be related to too much cloud cover which is supported by the large spring cold bias of the 2m temperature (see Fig. 20) and the corresponding too little upward sensible heat flux. Originally it was thought that the underestimation of surface solar radiation may be related to a too large albedo but the snow-free albedo values over land (not shown) correspond well to the ones in the ERA data set. Despite the too cold temperatures the snow cover and the snowmelt (see Fig. 24) are simulated quite well which suggests that also the surface albedo is not responsible for the biases in the spring. As the latent heat flux is comparatively close to the ERA data, the SVATS seems to perform well in this region.

In an earlier version of the CHRM model (*Vidale et al.*, 2002), a large negative bias in surface solar radiation (up to -50 W/m^2 in May/June) was present. This bias has been clearly reduced (extreme of -20 W/m^2 in May) by the restoration of surface solar radiation, which had been strongly depressed by the low level clouds diagnosed by the *Slingo* (1987) cloud scheme with the enhanced summer moisture flux. This was accomplished by implementing the *Xu and Randall* (1996) cloud diagnostics, which mainly affect the liquid water path seen by the radiation rather than the distribution of cloud types which were not substantially modified. Concurrently, the biases in other components of the surface energy balance were also reduced, in particular the negative sensible heat bias in the summer.

5.2.4. HadRM3H

HadRM3H overestimates the precipitation and evapotranspiration except during the summer (Fig. 32). In the spring, the comparatively large evapotranspiration bias causes too little convergence of moisture in the atmosphere from other regions. As the snowmelt almost completely infiltrates into the soil (cf. Sect. 4.1), thereby causing the large negative spring runoff bias, the soil is too wet which results in the overestimated evapotranspiration. Fig. 33 doesn't show an overestimation of latent heat flux compared to ERA. This can be explained by the fact that the ERA surface scheme behaves very similarly in the unrealistic treatment of the snowmelt (see *Hagemann and Dümenil Gates*, 2001). Thus, the latent heat flux and the evaporation of ERA are highly unreliable in regions and months where the snow is melting. Since the 2m temperature in the spring is simulated well, the snow albedo may be too low. This is supported by too much downward surface solar radiation and too much upward surface thermal radiation during the winter.

5.2.5. REMO

For REMO, the biases of the hydrological cycle (Fig. 34) are similar to HIRHAM (see Sect. 5.2.1) except for the fact that REMO simulates less evapotranspiration and more precipitation during the winter and the early spring. The deviation of the upward surface thermal radiation to ERA data (Fig. 35) closely follows the 2m temperature bias (Fig. 20), with too large values in the summer and too low values in the winter and early spring. The temperature bias may be caused by deficits in the simulation of clouds, as the too large downward surface solar radiation in the summer may be related to an underestimation of cloud cover and the too little surface solar radiation in the spring and autumn may be related to an overestimation of cloud cover.

Another reason for the temperature bias may be the absence of a seasonal cycle in the vegetation in REMO. HIRHAM, where a seasonal variation of LAI and vegetation ratio is implemented, shows almost no temperature bias in the Baltic Sea catchment (Fig. 20). An implementation of a seasonal vegetation cycle would lead to an increase in summer evapotranspiration (cooling of the surface) and a decrease in winter evapotranspiration (less cooling of the surface) so that the temperature bias would be reduced.

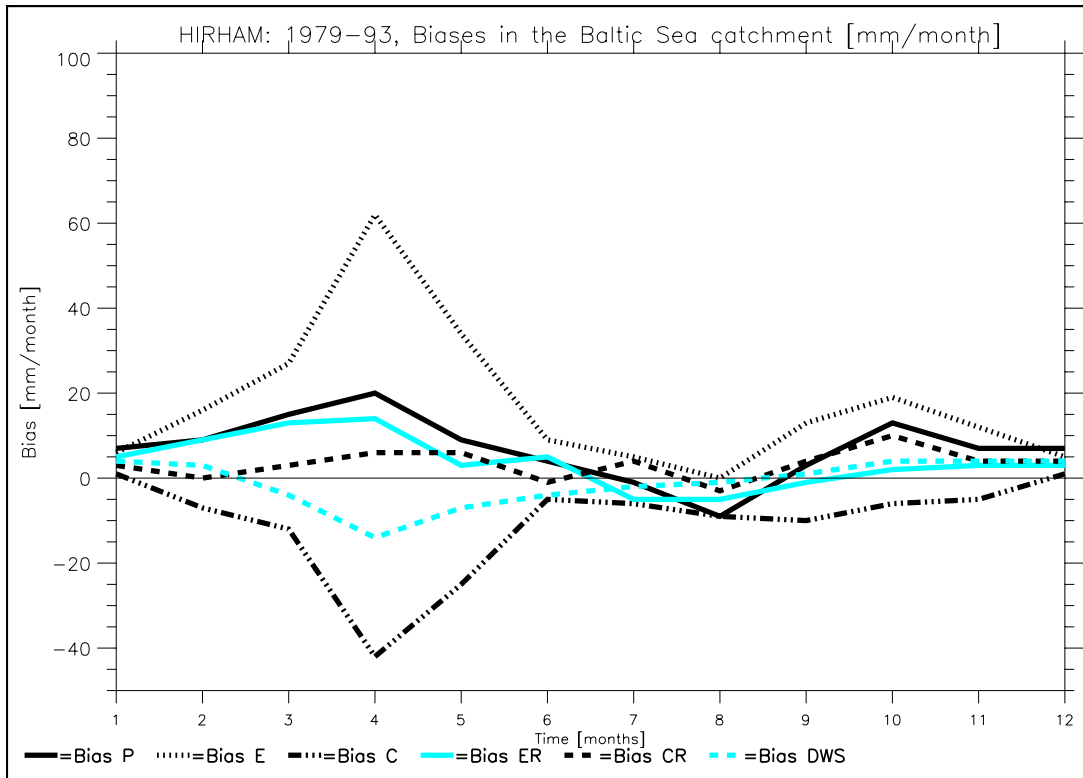


Fig. 26. Biases in the hydrological cycle of the HIRHAM simulation (1979-93) in mm/month over the Baltic Sea catchment. P = precipitation, E = evapotranspiration, C = convergence, ER = evapotranspiration (using ERA data), CR = convergence (using ER), DWS = Storage change = ΔWS

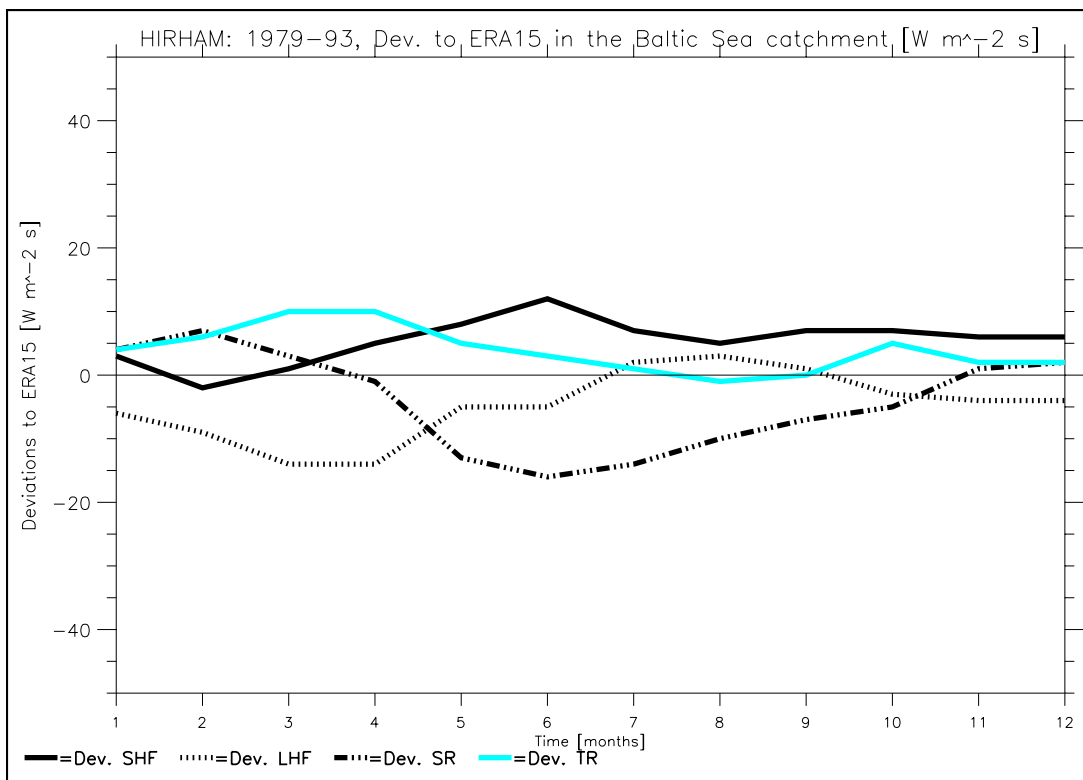


Fig. 27. Deviations from ERA of the surface energy fluxes of the HIRHAM simulation (1979-93) in $W m^{-2} s$ over the Baltic Sea catchment
 SHF = sensible heat flux, LHF = latent heat flux, SR = surface solar radiation, TR = surface thermal radiation

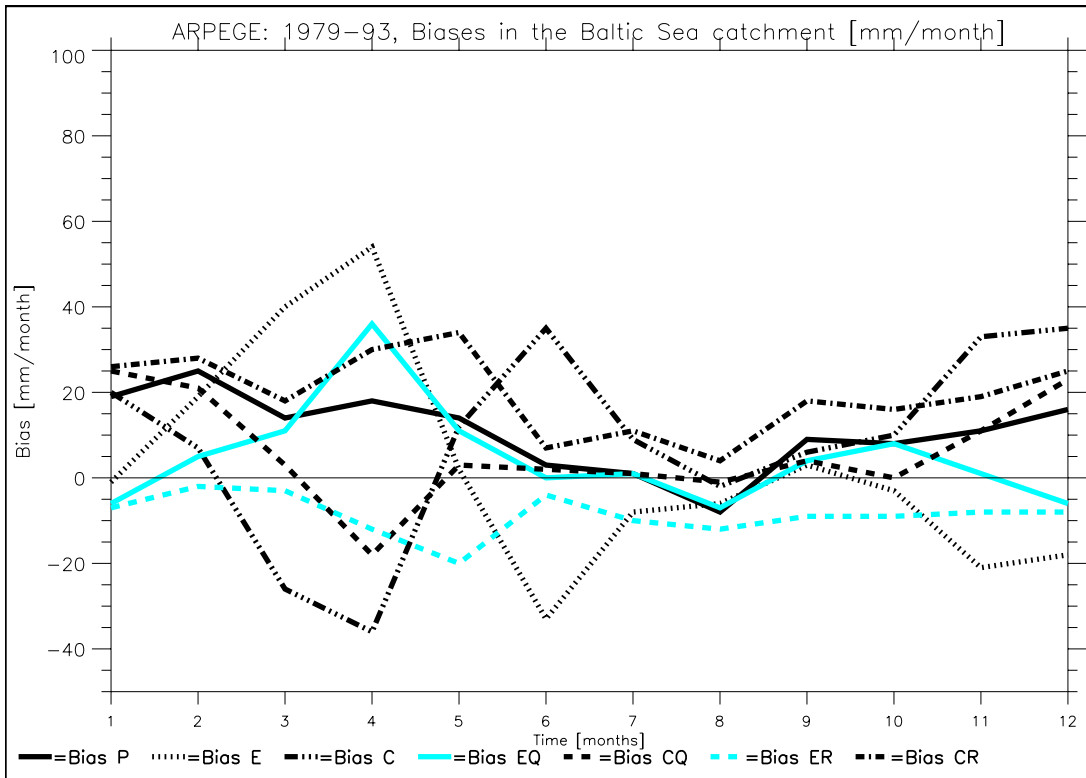


Fig. 28. Biases in the hydrological cycle of the ARPEGE simulation (1979-93) in mm/month over the Baltic Sea catchment. P = precipitation, E = evapotranspiration, C = convergence, EQ = evapotranspiration (2nd estimate), CQ = convergence (2nd estimate), ER = evapotranspiration (using ERA data), CR = convergence (using ER)

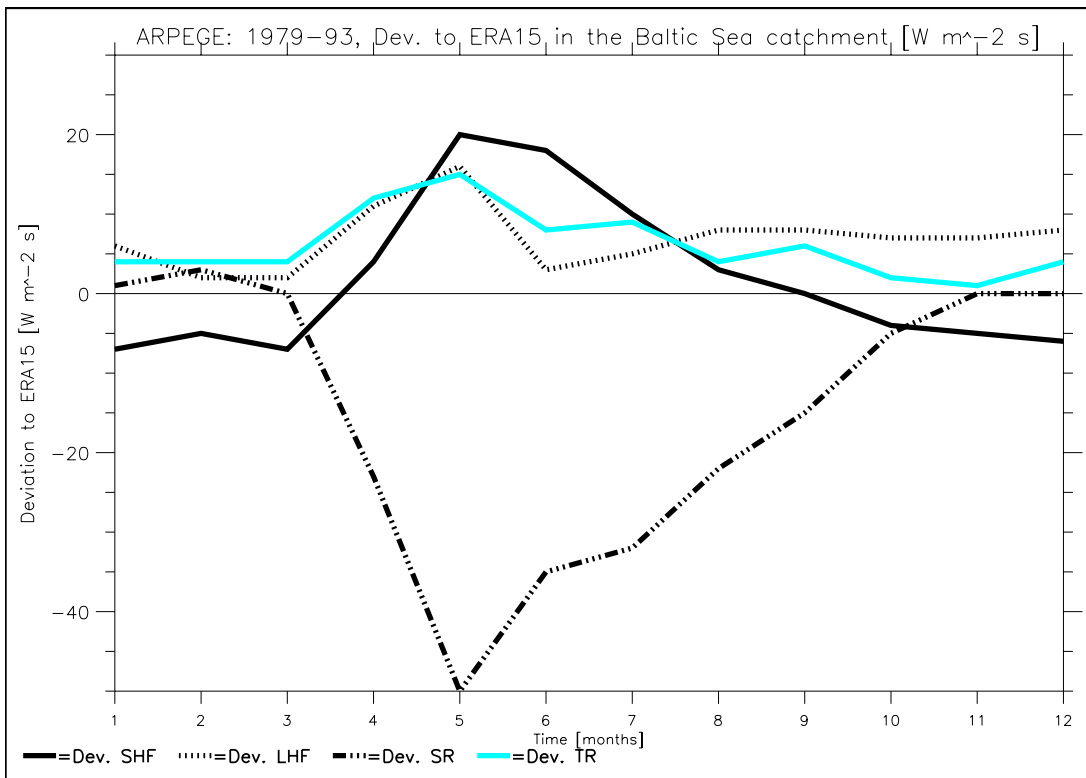


Fig. 29. Deviations from ERA of the surface energy fluxes of the ARPEGE simulation (1979-93) in Wm⁻²s over the Baltic Sea catchment
SHF = sensible heat flux, LHF = latent heat flux, SR = surface solar radiation, TR = surface thermal radiation

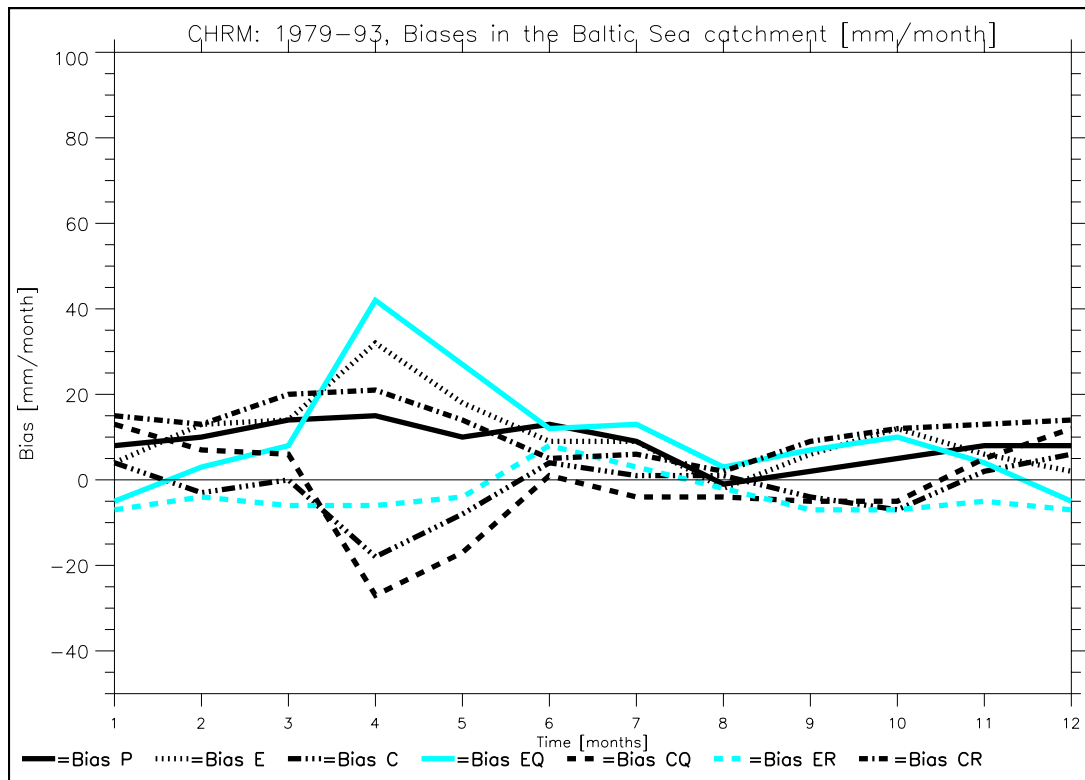


Fig. 30. Biases in the hydrological cycle of the CHR simulation (1979-93) in mm/month over the Baltic Sea catchment. P = precipitation, E = evapotranspiration, C = convergence, EQ = evapotranspiration (2nd estimate), CQ = convergence (2nd estimate), ER = evapotranspiration (using ERA data), CR = convergence (using ERA)

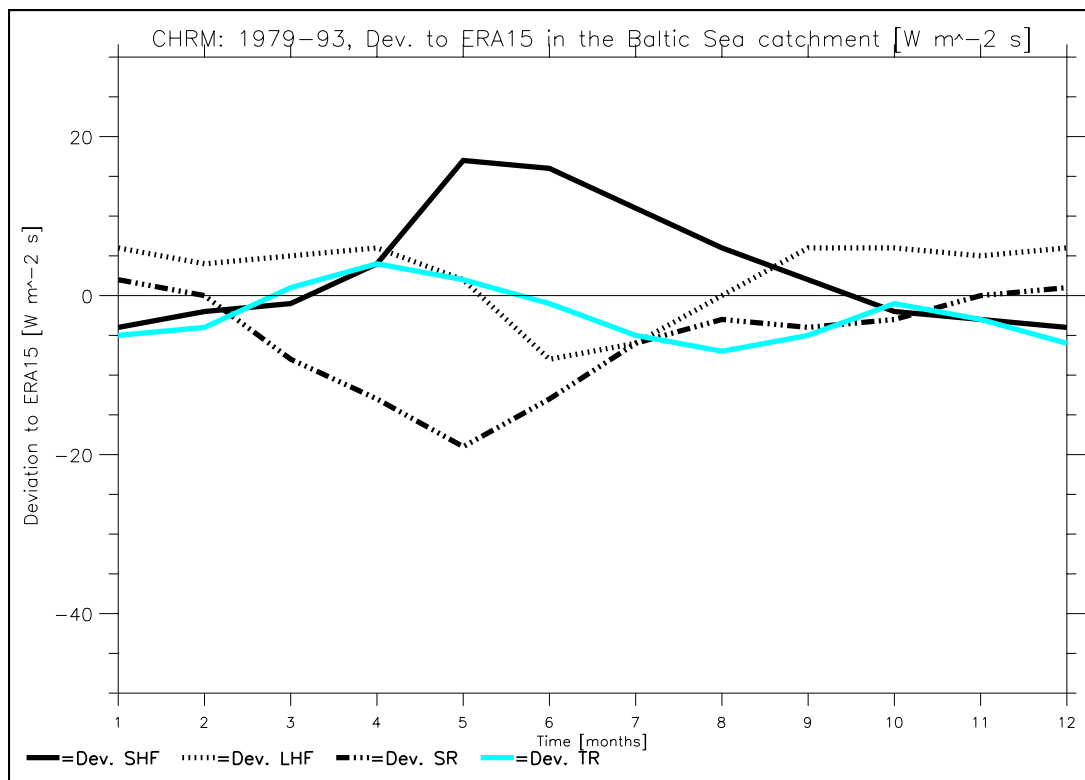


Fig. 31. Deviations from ERA of the surface energy fluxes of the CHR simulation (1979-93) in Wm⁻²s over the Baltic Sea catchment
SHF = sensible heat flux, LHF = latent heat flux, SR = surface solar radiation, TR = surface thermal radiation

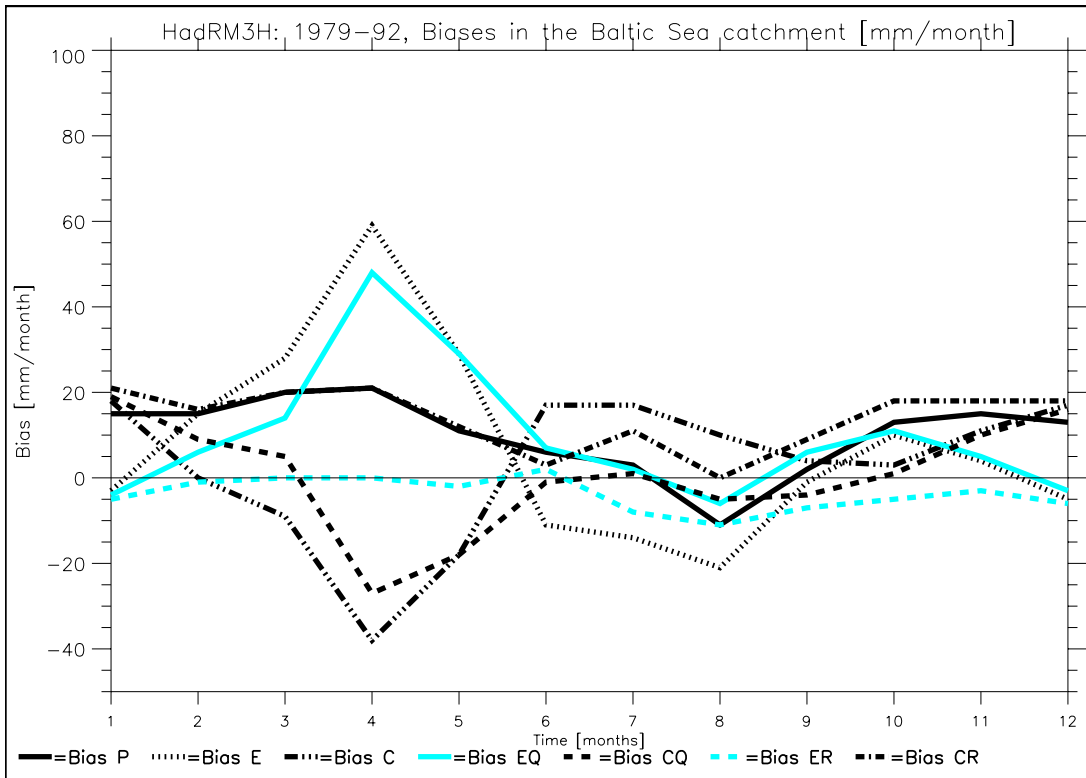


Fig. 32. Biases in the hydrological cycle of the HadRM3H simulation (1979-92) in mm/month over the Baltic Sea catchment. P = precipitation, E = evapotranspiration, C = convergence, EQ = evapotranspiration (2nd estimate), CQ = convergence (2nd estimate), ER = evapotranspiration (using ERA data), CR = convergence (using ER)

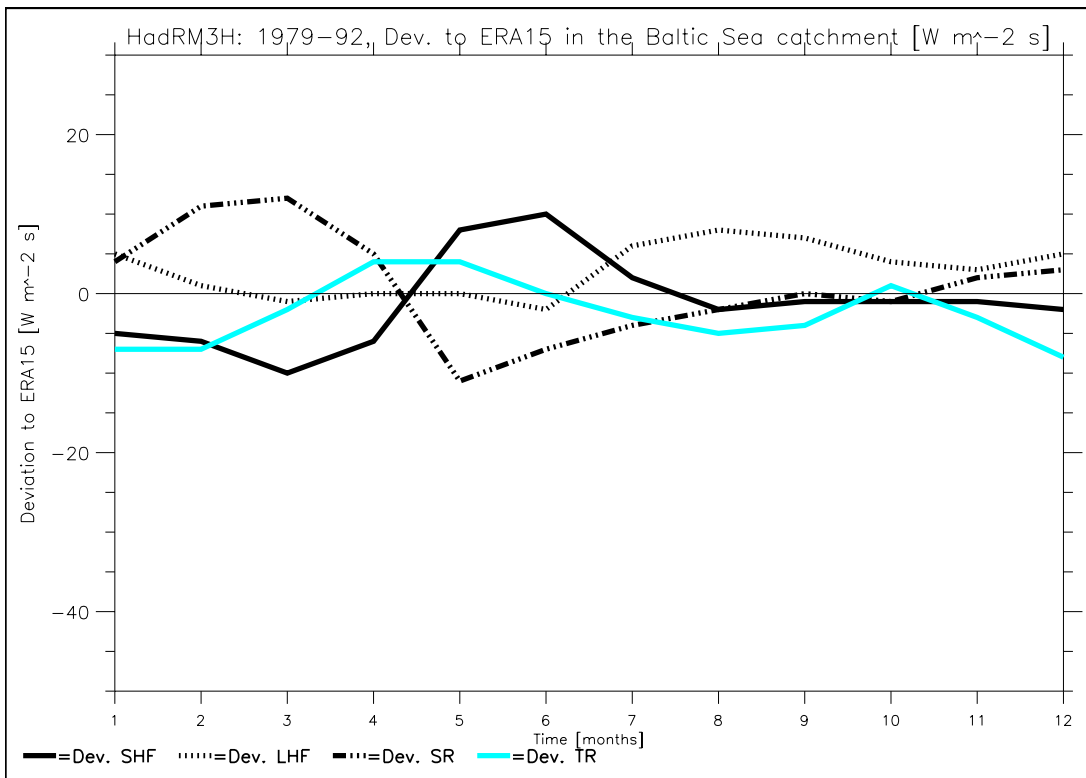


Fig. 33. Deviations from ERA of the surface energy fluxes of the HadRM3H simulation (1979-92) in $W m^{-2} s$ over the Baltic Sea catchment
SHF = sensible heat flux, LHF = latent heat flux, SR = surface solar radiation, TR = surface thermal radiation

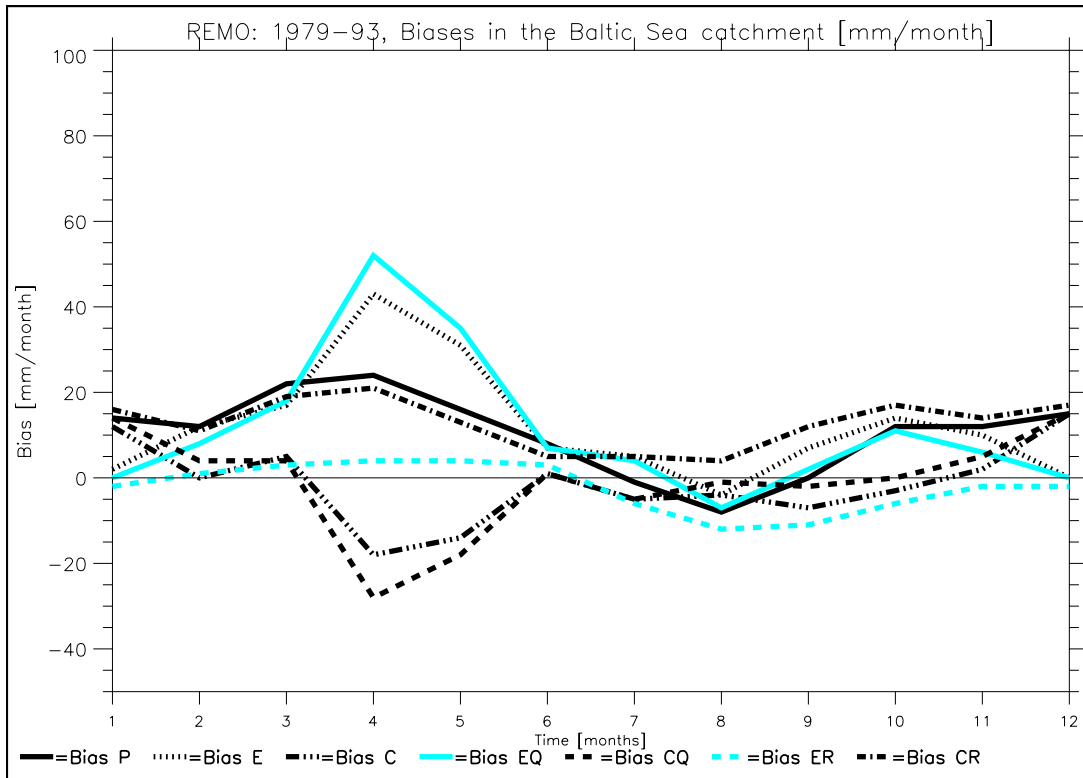


Fig. 34. Biases in the hydrological cycle of the REMO simulation (1979-93) in mm/month over the Baltic Sea catchment. P = precipitation, E = evapotranspiration, C = convergence, EQ = evapotranspiration (2nd estimate), CQ = convergence (2nd estimate), ER = evapotranspiration (using ERA data), CR = convergence (using ERA)

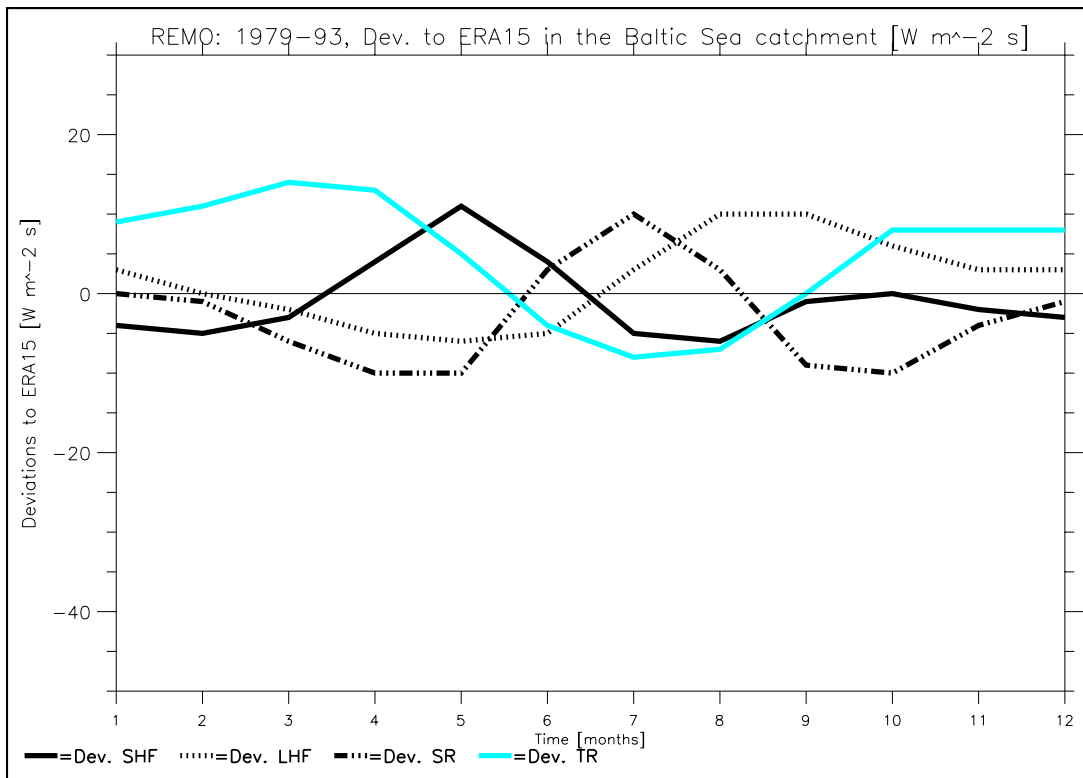


Fig. 35. Deviations from ERA of the surface energy fluxes of the REMO simulation (1979-93) in Wm⁻²s over the Baltic Sea catchment
SHF = sensible heat flux, LHF = latent heat flux, SR = surface solar radiation, TR = surface thermal radiation

6. Conclusions

In this study, the water and energy budgets simulated by five regional climate models applied over Europe were compared. It was focused on two large catchments with different climates. For the Baltic Sea catchment that represents a maritime climate, all models show a similar simulation of precipitation which is overestimated throughout the year except during the summer, and which represents the annual cycle of precipitation quite well. As the advection of moisture does not seem to be a major error source for this overestimated precipitation, it is probably caused by the internal model parameterizations, such as the large-scale condensation and the convection schemes. Thus, these internal parameterizations should be the focus of future studies to improve the models.

For the Danube catchment that represents a more continental climate, problems in the regional climate simulations are mainly induced by two different reasons. For ARPEGE and CHRM, the problems are related to deficiencies in the land surface parameterizations, while for HIRHAM, HadRM3H and REMO systematic errors in the dynamics are causing the main errors in the simulations. The prominent summer drying problem is a major feature of all models except ARPEGE.

As far as ARPEGE is concerned, the main characteristic of its systematic error is the too large snow accumulation in winter. It results in a too large runoff in spring associated with too cold spring and autumn temperatures. However, the model is not excessively cold or wet in winter (at least in the two basins). Thus, the error comes from the snow parameterization which is too snow-conservative by maintaining high albedo and weak conductivity. In earlier versions of the model, the snow cover was underestimated over Europe and the recent modifications of the scheme have led to the opposite defect. The snow-albedo feedback is very sensitive and small changes produce large effects.

For CHRM, the major source for its summer drying problem seems to be the force-restore soil model which simulates a too weak diurnal cycle that may be also shifted in time. It also cannot retain sufficient memory of the summer heat storage which may lead to the winter cold bias. Further tests with a more advanced SVATS, coupled to a multi-level diffusive soil model, capable of retaining long term soil heat history, will be performed to address this issue.

For HIRHAM, HadRM3H, and REMO, the summer drying problem is induced by problems in the general circulation of the models where too little moisture is advected into the region (or too much divergence occurs, respectively). This leads to a lack in cloud cover which influences the surface energy fluxes. This dynamical problem of erroneous moisture transports is a large-scale problem that seems to be independent of the domain size. As it also occurs in several models it might be that deficient features in the dynamic part of CHRM and ARPEGE may also exist which are only overlaid by the systematic errors in the surface parameterizations of these two models. This has to be investigated when the surface parameterizations of both models are revised.

As it is assumed that the erroneous moisture transports seen in HIRHAM, HadRM3H and REMO are caused by errors in the general circulation of the atmosphere, in spite of ERA boundary conditions used, it is important to find the reason for these errors. In particular it may be that these errors will be larger in real climate simulations with boundary conditions from GCM simulations instead of reanalyses (see e.g. *MERCURE*, 2002). A more precise estimation of the causes of the errors revealed in the present studies may be carried out by

systematic initial tendency error (SITE) estimates (*Machenhauer and Kirchner, 2000*) using ERA data or the new 40 years ECMWF re-analysis data (ERA40) that are currently under production. SITE estimates can be used to assess errors in the model physics or to find missing external forcings. Alternatively, as demonstrated by *Jones et al. (2002)* for HadRM3H, a more in depth analysis of the hydrological cycle over the region can help to isolate the precise causes of the error from the feedbacks which help to maintain it. In the present study we came closer to an understanding of the long lasting summer drying problem in regional climate simulations over Europe. However, we still do not fully understand it, and we have not managed to eliminate it completely. Further studies along the lines suggested should provide a complete understanding of the error and indicate model improvements required to remove it in future model configurations.

Acknowledgements. We would like to thank Michael Botzet and Ralf Podzun from the MPI in Hamburg, Jens H. Christensen and Jan-Peter Schulz from the DMI in Copenhagen, David Hassell and Ruth Taylor from the Hadley Centre in Bracknell for their close cooperation within the MERCURE project which has been the basis of the results presented in this paper. This study was supported by funding from the European Union within the MERCURE (Modelling European Regional Climate: Understanding and Reducing Errors) project (contract No. ENV4-CT97-0485).

References

- BALTEX (1995) Baltic sea experiment, BALTEX. Initial implementation plan. *International BALTEX Secretariat. Publ. 2*, Geesthacht
- Beljaars, ACM., and Viterbo, P. (1998) Role of the boundary layer in a numerical weather prediction model, Ed.: AAM Holstlag and Pg Duynkerke: *Clear and Cloudy Boundary Layers*, Amsterdam, 3722 pp.
- Bengtsson, L. (2001) Numerical modelling of the energy and water cycle of the Baltic Sea, *Meteorology and Atmospheric Physics* **77**, 9-17
- Bonan, G.B. (1996) A land surface model (LSM version 1.0) for ecological, hydrological, and atmospheric studies: Technical description and user's guide, *NCAR Technical Note NCAR/TN-417+STR*, National Center for Atmospheric Research, Boulder, CO
- Christensen, J.H., Christensen, O.B., Lopez, P., van Meijgaard, E., and Botzet, M. (1996) The HIRHAM 4 regional atmospheric climate model, *DMI*, Scientific Report **96-4** (Available from DMI, Lyngbyvej 100, DK-2100 Copenhagen Ø)
- Christensen O.B., Christensen, J.H., Machenhauer, B. and Botzet, M. (1998) Very high-resolution regional climate simulations over Scandinavia - Present climate, *J. Climate* **11**, 3204-3229
- Christensen, J.H., Christensen, O.B., Schulz, J-P., Hagemann, S., and Botzet, M. (2001) High resolution physiographic data set for HIRHAM 4: An application to 50 km horizontal resolution domain covering Europe, *DMI*, Technical Report **01-15 4** (Available from DMI, Lyngbyvej 100, DK-2100 Copenhagen Ø).
- Cox, P.M., Betts, R.A., Bunton, C.B., Essery, R.L.H., Rowntree, P.R. and Smith, J. (1999) The

- impact of new land surface physics on the GCM simulation of climate and climate sensitivity. *Clim. Dyn.* **15**, 183-203
- Cusack, S., Edwards, J. M., and Kershaw, R. (1999) Estimating the subgrid variance of saturation, and its parametrization for use in a GCM cloud scheme. *Q. J. R. Met. Soc.* **125**, 3057-3076
- Davies, H.C. (1976) A lateral boundary formulation for multi-level prediction models. *Quart. J. R. Meteor. Soc.* **102**, 405-418
- Déqué, M., Marquet, P., and Jones, R.G. (1998) Simulation of climate change over Europe using a global variable resolution general climate model, *Clim. Dyn.* **14**, 173-189
- Dickinson, R.E. (1984) Modeling evapotranspiration for the three-dimensional global climate models. Climate Processes and Climate Sensitivity, *Geophys. Monogr.* **29**, Amer. Geophys. Union, Hansons, J.E. and Takahashi, T., 58-72
- Dickinson, R.E., Henderson-Sellers, A., and Kennedy, P.J. (1993) Biosphere-Atmosphere Transfer Scheme (BATS) Version 1e as coupled to the NCAR community climate model, *NCAR Technical Note* **387**, Boulder, Colorado
- Dümenil, L., and Todini, E. (1992) A rainfall-runoff scheme for use in the Hamburg climate model, Ed.: J.P. Kane: *Advances in Theoretical Hydrology - a Tribute to James Dooge*, Elsevier Science Publishers, 129-157
- Foster, D.J., and Davy, R.D. (1988) Global snow depth climatology, *USAFETAC/TN-88/006*, Scott Air Force Base, Ill.
- Gibson, J.K., Kållberg, P., Uppala, S., Hernandez, A., Nomura, A., and Serrano, E. (1997) Era description, *ECMWF Re-Analysis Project Report Series* **1**
- Gregory, J.M. (1999) Representation of the radiative effect of convective anvils. *HCTN* **9**, Hadley Centre, The Met. Office, Bracknell, UK
- Hagemann, S. (2002) An improved land surface parameter dataset for global and regional climate models, *Max-Planck-Institute for Meteorology*, Report **336**, Hamburg, Germany. (Report available electronically from: <http://www.mpimet.mpg.de/deutsch/Sonst/Reports/HTMLReports/289/>)
- Hagemann, S., Botzet, M., Dümenil, L., and Machenhauer, B. (1999) Derivation of global GCM boundary conditions from 1 km land use satellite data, *Max-Planck-Institute for Meteorology*, Report **289**, Hamburg, Germany. (Report available electronically from: <http://www.mpimet.mpg.de/deutsch/Sonst/Reports/HTMLReports/289/>)
- Hagemann, S., Botzet, M., and Machenhauer, B. (2001) The summer drying problem over south-eastern Europe: Sensitivity of the limited area model HIRHAM4 to improvements in physical parameterization and resolution, *Physics and Chemistry of the Earth, Part B*, **26**, 391-396
- Hagemann, S., and Dümenil, L. (1999) Application of a Global Discharge Model to Atmospheric Model Simulations in the BALTEX Region, *Nordic Hydrology* **30**, 209-230
- Hagemann, S., and Dümenil, L. (2001) Validation of the hydrological cycle of ECMWF and NCEP reanalyses using the MPI hydrological discharge model, *J. Geophys. Res.* **106**, 1503-1510
- Hulme, M., Conway, D., Jones, P.D., Jiang, T., Barrow, E.M., and Turney, C. (1995) Construction of a 1961-1990 European climatology for climate change modelling and

- impact applications, *Int. J. Climatol.* **15**, 1333-1363
- Jacob, D. (2001) A note to the simulation of the annual and inter-annual variability of the water budget over the Baltic Sea drainage basin, *Meteorology and Atmospheric Physics* **77**, 61-73
- Jacobsen, I. and Heise, E. (1982) A new economic method for the computation of the surface temperature in numerical models. *Beitr. Phys. Atm.* **55**, 128-141
- Jones, R.G., Murphy, J.M., and Noguer, M. (1995) Simulation of climate change over Europe using a nested regional climate model. I: Assessment of control climate, including sensitivity to location of lateral boundaries, *QJR Meteorol. Soc.* **121**, 1413-1449
- Jones, R.G., Taylor, R.S., and Buonomo, E. (2002). The new Hadley Centre regional climate modelling system: Performance and error analysis over Europe. In preparation.
- Kållberg, P., and Gibson, R., (1977) Multi level limited area forecasting using boundary zone relaxation, *GARP Programme on Numerical Experimentation*, Rep. **15**, 128 pp.
- Källén, E., Ed. (1996) HIRLAM documentation manual, system 2.5, *Swedish Meteorological and Hydrological Institute*, 126 pp. [Available from SMHI, S-60176, Norrköping, Sweden.]
- Kessler, E. (1969) On the distribution and continuity of water substance in atmospheric circulation models. *Meteor. Monographs* **10**, Americ. Meteor. Soc. Boston, MA
- Lin, Y.-L., Farley, R.D., and Orville, H.D. (1983) Bulk parameterization of the snow field in a cloud model. *J. Clim. Appl. Meteor.* **22**, 1065-1092
- Louis, J.F. (1979) A parametric model of vertical eddy fluxes in the atmosphere, *Bound.-Layer Meteor.* **17**, 187-202
- Louis, J.F., Tiedtke, M., and Geleyn, J.F. (1982) A short history of the operational PBL parameterization at ECMWF. *Proc. ECMWF Workshop on Boundary Layer parameterizations*, ECMWF, 59-79
- Lunardini, V.J. (1983) Heat transfer in cold climates. Van Nostrand reinhold, New York
- Lüthi, D., Cress, A., Davies, H.C., Frei, C., and Schär, C. (1996) Interannual variability and regional climate simulations, *Theor. Appl. Climatol.* **53**, 185-209
- Machenhauer, B., and Kirchner, I. (2000) Diagnosis of systematic initial tendency errors in the ECHAM AGCM using slow normal mode data assimilation of ECMWF reanalysis data, *CLIVAR Exchanges* **5** (4), 9-10
- Machenhauer, B., Windelband, M., Botzet, M., Jones, R.G., and Déqué, M. (1996) Validation of present-day regional climate simulations over Europe: Nested LAM and variable resolution global model simulations with observed or mixed layer ocean boundary conditions, *Max-Planck-Institute for Meteorology*, Report **191**, Hamburg, Germany.
- Machenhauer, B., Windelband, M., Botzet, M., Christensen, J.H., Déqué, M., Jones, R.G., Ruti, P.M., and Visconti, G. (1998) Validation and analysis of regional present-day climate and climate change simulations over Europe, *Max-Planck-Institute for Meteorology*, Report **275**, Hamburg, Germany. (Report available electronically from: <http://www.mpimet.mpg.de/deutsch/Sonst/Reports/HTMLReports/275/>)
- Majewski, D., and Schrodin, R. (1994) Short description of the Europa-Modell (EM) and Deutschland-Modell (DM) of the DWD, *Quarterly Bulletin* (April)
- Majewski, D., Liermann, D., Prohl, P., Ritter, B., Buchhold, M., Hanisch, T., Paul, G., Wergen, W., and Baumgardner, J. (2001) The global icosahedral-hexagonal grid point model GME -

- operational version and high resolution tests, *Mon. Wea. Rev.*, accepted.
- Mellor, G.L., and Yamada, T. (1974) A hierarchy of turbulent closure models for planetary boundary layers. *J. Atmos. Sci.* **31**, 1791-1806
- MERCURE (2002) MERCURE - Final project report, Ed.: Jones, R.G. and Co-Workers, EU, Brussels, Belgium
- Murphy, J.M., Jones, R.G., Hassell, D.C., and Woodage, M., (2002) A high resolution atmospheric GCM for the generation of regional climate scenarios. In preparation.
- Patterson, K.A. (1990) Global distributions of total and total-avaiable soil water-holding capacities, Master's thesis, University of Delaware, Newark, DE
- Pope, V.D., Gallani, M., Rowntree, P.R., and Stratton, R.A. (2000) The impact of new physical parametrizations in the Hadley Centre climate model - HadAM3. *Clim. Dyn.* **16**, 123-146
- Ritter, B, and Geleyn, J.F. (1992) A comprehensive radiation scheme for numerical weather prediction models with potential applications in climate simulations. *Mon. Wea. Rev.* **120**, 303-325
- Roeckner, E., Arpe, K., Bengtsson, L., Christoph, M., Claussen, M., Dümenil, L., Esch, M., Giorgetta, M., Schlese, U., and Schulzweida, U. (1996) The atmospheric general circulation model ECHAM-4: model description and simulation of present-day climate, *Max-Planck-Institute for Meteorology*, Report **218**, Hamburg, Germany
- Sellers, P.J., Los, S.O., Tucker, C.J., Justice, C.O., Dazlich, D.A., Collatz, G.J., and Randall, D.A. (1994) A global 1 by 1 degree NDVI data set for climate studies. Part 2: The generation of global fields of terrestrial biophysical parameters from the NDVI. *Int. J. Remote Sens.* **15(17)**, 3519-3545
- Shapiro, R., (1970) Smoothing, filtering and boundary effects, *Rev. Geophys. Space Phys.* **8**, 359-387
- Simmons, A.J., and Burridge, D.M. (1981) An energy and angular momentum conserving vertical finite-difference shceme and hybrid vertical coordinates. *Mon. Wea. Rev.* **109**, 758-766.
- Slingo, J.M. (1987) The development and verification of a cloud prediction scheme for the ECMWF model, *Quart. J. Roy Meteor. Soc.* **116**, 435-460
- Tiedtke, M. (1989) A comprehensive mass flux scheme for cumulus parameterization in large-scale models. *Mon. Wea. Rev.* **117**, 1779-1800
- Vidale, P.L., Lüthi, D., Frei, C., Seneviratne, S., and Schär, C. (2002) Physical processes affecting the seasonal and inter-annual variations of the European water cycle. *Quart. J. Roy Meteor. Soc.*, in preparation
- Wild, M, Ohmura, A., Gilgen, H., and Roeckner, E. (1995) Validation of GCM simulated radiative fluxes using surface observations, *J. Clim.* **8**, 1309-1324
- Wild, M.A., Dümenil, L., and Schulz, J.-P. (1996) Regional climate simulation with a high resolution GCM: surface hydrology, *Clim. Dyn.* **12**, pp. 755-774
- WMO (World Meteorological Organization) (1988) Concept of the Global Energy and Water Cycle Experiment. Technical report, WCRP-5, WMO/TD No. 215, Geneva, Switzerland
- Xu, K.-M., and Randall, D. (1996) A semiempirical cloudiness parameterization of ruse in climate models. *J. Atmos. Sci.* **53**, 3084-3102